ELSO: A New Enhanced Light Spectrum Optimization Algorithm

Jing Wang, Yukun Wang*, and Zhongfeng Li

Abstract—**The Light Spectrum Optimizer (LSO) is a novel metaheuristic algorithm inspired by the natural phenomenon of rainbow spectrum formation. To address the limitations of slow convergence, proneness to local optima entrapment, and insufficient population diversity inherent in LSO, this study proposes an Enhanced Light Spectrum Optimizer (ELSO). The proposed enhancements include: (1) Population initialization via the Logistic chaotic mapping generates diverse distribution patterns, thereby enhancing global search capabilities and accelerating convergence speed; (2) Integrating the Cauchy mutation mechanism improves population diversity by leveraging its heavy-tailed distribution, thereby enhancing global exploration and avoiding premature convergence to local optima; (3) Lévy flight trajectory adoption to optimize the exploration-exploitation balance, thereby improving performance in complex optimization scenarios. Furthermore, the Fitness-Distance Constraint (FDC) method is synergistically combined with ELSO to develop the FDC-ELSO variant, significantly enhancing constraint-handling capabilities. Comprehensive evaluations were conducted using CEC2017 benchmark functions and four classical engineering optimization problems (spring system design, gearbox design, wireless sensor network coverage optimization, and arch bridge structural design). Statistical validation was conducted using the Friedman rank test and Wilcoxon signed-rank test. The results demonstrated that ELSO and FDC-ELSO exhibit superior performance metrics compared to existing algorithms. The proposed frameworks demonstrate strong practical applicability across multiple engineering domains, confirming their theoretical validity and engineering value.**

Index Terms—**Light spectral optimizer, Logistic chaotic mapping, Cauchy mutation, Lévy flight**

I. INTRODUCTION

Optimization are generally divided into two types: unconstrained optimization and constrained optimization. Unconstrained optimization problems involve no restrictions during solution searching, while constrained optimization problems require solutions to meet specific equality or inequality constraints. Both unconstrained and constrained optimization problems are pervasive in mathematics, engineering, and economics. However, as these problems become increasingly complex, traditional analytical methods often become impractical or inadequate. In response, meta-heuristic algorithms have gained prominence, valued for their strong global search capabilities and adaptability to various problem domains. Classic algorithms such as Particle Swarm Optimization (PSO) [1], Genetic Algorithm (GA) [2], and Differential Evolution (DE) [3] have achieved outstanding results in a wide range of optimization tasks and have inspired the development of numerous improved variants. Nonetheless, with increasing problem complexity, these traditional algorithms frequently encounter limitations, including premature convergence to local optima and reduced convergence efficiency. This has led to significant research focus on developing more efficient and adaptable meta-heuristic algorithms for handling both unconstrained and constrained optimization challenges [4]. Such advancements hold substantial theoretical value while providing critical technical solutions for real-world engineering optimization needs.

The Light Spectrum Optimizer (LSO), proposed by Abdul-Basset in 2022, is inspired by the formation of rainbows through light scattering in raindrops. Owing to its conceptual simplicity and impressive performance in global optimization tasks, this algorithm has attracted considerable attention within the computational intelligence community. Subsequent research has focused on further expanding and refining the LSO's capabilities. For instance, Reda Mohamed developed the Binary Light Spectrum Optimizer (BLSO), which enhances combinatorial optimization and demonstrates improved performance on the 0-1 Knapsack Problem (KP01) and the Multidimensional Knapsack Problem (MKP) [5]; In another example, Thiyagu Thulasi integrated the LSO with a Multi-Stage Convolutional Neural Network (MSCNN), creating a hybrid MSCNN-LSO framework for hyperparameter optimization in Internet of Things (IoT) healthcare systems; this integration significantly improves intrusion detection accuracy in medical environments [6]; Additionally, Safaa Saber's Improved Light Spectrum Optimizer (ILSO) advances photovoltaic modeling by achieving precise parameter estimation for Triple-Diode Models (TDM), outperforming conventional approaches [7]. Despite considerable progress, LSO still has several limitations when tackling complex optimization scenarios. These include insufficient population diversity, a tendency to converge prematurely to suboptimal solutions, and slow convergence rates. Collectively, these issues limit its effectiveness in high-dimensional or multi-modal problem spaces.

To address the aforementioned limitations in existing algorithms, this paper proposes the Enhanced Light

Manuscript received March 5, 2025; revised July 4, 2025.

This work was supported by Liaoning Provincial Joint Funds Project of China (Grant No. 2023-MSLH-323).

Jing Wang is a postgraduate student of School of Electronic and Information Engineering, University of Science and Technology Liaoning, Anshan, Liaoning 114051, PR China (e-mail: 17660189676@163.com).

Yukun Wang is an associate professor of School of Electronic and Information Engineering, University of Science and Technology Liaoning, Anshan, Liaoning 114051, PR China (Corresponding author to provide phone: 86-0412-5929699; e-mail: wyk410@ustl.edu.cn).

Zhongfeng Li is an associate professor of School of Electrical Engineering, Yingkou Institute of Technology, Yingkou, Liaoning, PR China (e-mail: afeng0601@163.com).

Spectrum Optimizer (ELSO). ELSO improves population diversity, global search ability, and the capacity to escape local optima through three strategies: Logistic chaotic mapping, Cauchy mutation, and Lévy flight mechanisms. Moreover, the incorporation of the FDC method further enhances ELSO's performance in constrained optimization problems. This research aims to offer a more efficient solution approach for both unconstrained and constrained optimization challenges.

The remainder of this paper is structured as follows: Section 2 introduces the standard Light Spectrum Optimizer, outlining its theoretical basis and core operational principles, along with systematic mathematical formulations. Section 3 provides an in-depth description of ELSO, covering its motivation, key enhancement strategies, and implementation details. The workflow of the algorithm is depicted using a standardized flowchart. Section 4 establishes a standardized parameter configuration framework based on the CEC 2017 benchmark suite. This framework enables a comprehensive evaluation of algorithmic performance by validating enhancement strategies and analyzing parameter sensitivity. Section 5 presents a qualitative comparison between LSO and ELSO, a quantitative comparison of ELSO against other algorithms using the Friedman test and Wilcoxon signed-rank test, and highlights the advantages of ELSO. Section 6 discusses engineering applications from two perspectives: solving unconstrained optimization problems and addressing constrained optimization cases. Finally, Section 7 concludes the paper by summarizing the technical contributions of ELSO supported by experimental validation, critically discussing current research limitations, and suggesting future extensions for discrete and multi-objective optimization problems.

II. Introduction of Standard Spectrum Optimization Algorithm

The rainbow spectrum, a meteorological phenomenon produced by the dispersion of light, inspires the design of the LSO [8]. Its mathematical framework can be summarized as follows:

A. Initialization

Initialization involves the stochastic generation of candidate solutions at the commencement of the search process. The LSO algorithm's initialization procedure is mathematically defined as follows:

$$X^0 = LB + RV_1(UB - LB) \tag{1}$$

Where X^0 denotes the initial solution, and LB and UB lower and upper boundaries of the search space. A random number RV_1 is generated, uniformly distributed within the interval ([0, 1]). Each color ray corresponds to a candidate solution with a dispersion angle between 40° and 42°, and a refractive index defined as:

$$k^r = k^{red} + RV_1(k^{violet} - k^{red}) \tag{2}$$

Where $k^{red} = 1.331$.

B. Exploration phase

After determining the ray direction, a random probability p between 0 and 1 is generated, which is then used to construct the candidate solution. Specifically, if p is less than another random value between 0 and 1, a new candidate solution is generated:

$$X_{i+1}(t) = X_i(t) + \varepsilon RV_1^n GI\left(X_{L1}(t) - X_{L3}(t)\right) \times \left(X_{r1}(t) - X_{r2}(t)\right) \tag{3}$$

Otherwise, the new candidate solution is generated as:

$$X_{i+1}(t) = X_i(t) + \varepsilon RV_2^n GI\left(X_{L2}(t) - X_{L3}(t)\right) \times \left(X_{r3}(t) - X_{r4}(t)\right) \tag{4}$$

Where $X_{i+1}(t)$ is the newly generated candidate solution and $X_i(t)$ is the current candidate solution. r_1, r_2, r_3, r_4 are the indices of four solutions randomly selected from the current population. RV_1^n and RV_2^n are vectors of uniformly distributed random numbers in [0,1]. ε is the scaling factor computed by Equation (5). GI is an adaptive control parameter obtained from the inverse incomplete gamma function, as defined by Equation (6).

$$\varepsilon = a \times RV_3^n \tag{5}$$

Where RV_3^n is a standard normal random vector (with mean 0 and standard deviation 1), and a is an adaptive parameter calculated by the following equation:

$$GI = a \times r^{-1} \times P^{-1}(a,1) \tag{6}$$

GI is an adaptive control parameter [9]. R is a uniformly distributed random variable in [0, 1]. During the optimization process, R undergoes mathematical inversion to activate the exploration operator. This operation generates a real number exceeding 1. As a result, the current solution is displaced to an unexplored region within the search domain, enhancing the discovery of better solutions. P^{-1} represents the inverse incomplete gamma function applied to parameter a.

$$A = RV_2\left(1 - \left(\frac{t}{T_{\max}}\right)\right) \tag{7}$$

Where t represents the current iteration count, RV_2 denotes a uniformly distributed random variable in [0,1], and $T_{\max}$ specifies the maximum function evaluation cycles. When the input dimension exceeds 0.5, this inverse incomplete gamma function produces high-range values spanning 0.8 to 5.5, otherwise, it generates subunitary values approaching zero.

C. Exploitation phase

The exploitation phase enhances the algorithm's exploration capability through directional search guidance toward the current optimum or a randomly sampled candidate solution. This mechanism enables the expansion of the search region around the current solution, thereby improving solution quality, but it may also reduce the convergence speed of LSO. To balance convergence speed and solution quality, an adaptive strategy is introduced in this paper: the current solution migrates toward the global optimum with a fixed probability β. The mathematical formulation of this spatial distribution is presented in Equation (8):

$$X_{i+1}(t) = X_i(t) + RV_3 \times \left(X_{r1}(t) - X_{r2}(t) \right) + RV_4^n \times \left(R < \beta \right) \times \left(X^* - X_i(t) \right) \tag{8}$$

Where X^* denotes the current global optimum, Xr_1 and Xr_2 represent uniformly sampled candidate solutions. RV_3、RV_4^n contains a uniformly distributed random variable in [0,1]. In the second scattering phase, directional guidance vectors are generated at the updated positions using the historical best solution and the current solution, as described in Equation (9).

$$X_{i+1}(t) = 2\cos\left(\pi \times r_1\right)\left(X^*\right)\left(X_i(t)\right) \tag{9}$$

Where r_1 represents a uniformly distributed random variable in [0,1]. Π denotes the mathematical constant for the circle circumference ratio. The phase transition between primary and secondary scattering processes occurs with a fixed probability Pe as defined in the following equation:

$$X_{i+1}(t) = \begin{cases} Eq.(8) & if R < P_e \\ Eq.(9) & Otherwise \end{cases} \tag{10}$$

Where R represents a uniformly distributed random variable in [0,1], a novel candidate solution is generated through stochastic recombination of the randomly sampled parent and the current solution, marking the final scattering stage as defined in Equation (11):

$$X_{i+1}(t) = \left(X_{r1}^p + \left|RV_5\right| \times \left(X_{r2}(t) - X_{r3}(t) \right) \right) \times U + \left(1 - U\right) + \left(1 - U\right) \times X_i(t) \tag{11}$$

Where RV_5 represents a standard normal random variable (μ= 0, σ = 1), and U denotes a uniformly distributed random vector in [0,1].

III. The Proposed Enhanced Spectral Light Optimization Algorithm (ELSO)

To address the inherent limitations of conventional LSO algorithms-such as slow convergence rates and susceptibility to local optima-the ELSO framework introduces three enhancement strategies, as summarized in Table I.

A. *Logistic chaotic mapping*

Logistic chaotic mapping-based enhancement strategies are widely adopted in metaheuristic optimization. In this study, Logistic chaotic mapping is incorporated into ELSO

TABLE I
IMPROVEMENT STRATEGIES

No.	Improvement strategies
1	Logistic chaotic mapping
2	Cauchy mutation
3	Lévy flight

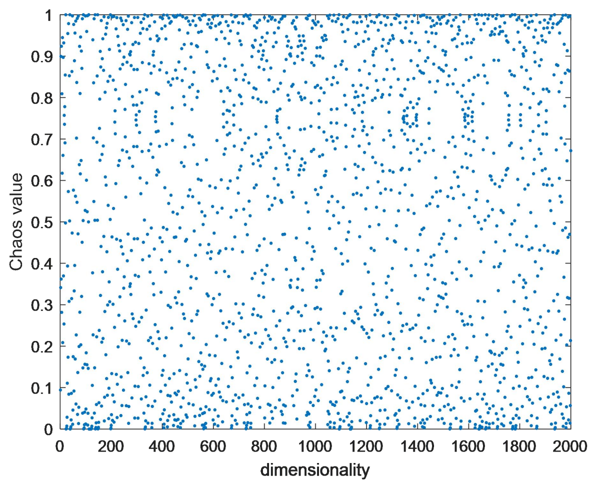

Fig. 1 Mapping graph

to generate *n_pop* initial population vectors at the population initialization phase [10]. Due to its ergodicity within the (0, 1) interval, Logistic chaotic mapping exhibits pseudo-random behavior, which helps to ensure population diversity by uniformly distributing the initial solutions throughout the search space. The mathematical formulation of the Logistic chaotic mapping used in this work is as follows:

$$Z_{n+1} = 4.0 * Z_n * \left(1 - Z_n\right) \tag{12}$$

Where Z_{n+1} and Z_n denote the population states at timesteps $t+1$ and t, respectively, and the parameter r is set to 4.0, the Logistic chaotic mapping demonstrates ergodicity in the (0,1) interval. This property ensures pseudo-random population distributions with uniform-like dispersion across the search space [35].

B. *Cauchy mutation*

The Cauchy mutation strategy is a widely used global search mechanism in evolutionary computation. This method enhances exploration ability and helps the algorithm escape local optima by introducing heavy-tailed noise from the Cauchy distribution [11].

During the update phase, Cauchy mutation is implemented through stochastic perturbations calculated as:

$$c = 0.5 * \exp\left(-1 * Iter / MaxIter\right) \tag{13}$$

Set a random number with a value range (0, 1), if $c > rand$, the positional update rule is defined in Equation (14):

$$X_{i,j}^{new} = X_{r1,j} + GI * \varepsilon * \ln(j) * \left(X_{r2,j} - X_{r3,j}\right) \tag{14}$$

Where $X_{i,j}^{new}$ represents the updated position of the i_th solution in the j_th dimension. GI denotes the global guidance factor, typically configured as either a constant or iteration-dependent parameter to adjust the magnitude of positional updates. ε is a small positive constant used to prevent numerical singularity $ln(j)$ when j=1.

The natural logarithm $ln(j)$ introduces dimension-wise weighting across search dimensions, while $X_{r2,j}$ and $X_{r3,j}$ denote the positional coordinates of two randomly selected solutions from the population in the j_th dimension [36].

If $c<rand$, the position update formula is:

$$X_{i+1}(t) = X_i(t) + GI * \ln(j) * R * (L_2 - L_3) \tag{15}$$

Where $X_{i+1}(t)$ represents the updated position vector of the i_th candidate, while X_i denotes its current state, R is a standard normal variate with dimensionality matching $X_i(t)$. L_2 and L_3 correspond to positional coordinates of two distinct population members randomly selected from the archive. The positional update rule applies when $rand<e$, $US>F*d$, the position update formula is:

$$\begin{aligned} X_{i+1}(t) &= US \times G_{best} + (1-US) \times X_{rand}(t) \\ &+ \cos(R \times 2\pi) \times (X_{rand1} - X_{rand2}) \end{aligned} \tag{16}$$

Among them:

$$F = \left| \frac{F_{best} - gbestValue}{gbestValue - \ln(Popsize)} \right| \tag{17}$$

$$US = rand(1, Dim) \tag{18}$$

$$d = \exp(-1 * Iter / MaxIter) \tag{19}$$

Where $Iter$ denotes the number of iterations, $MaxIter$ is the specified maximum number of iterations, and $PopSize$ represents the population size. $Fitness(i)$ indicates the fitness value of individual i, $Gbest$ refers to the positional coordinates of the optimal solution, and $gbestValue$ stores the global best fitness value. $X_{rand}(t)$ denotes the positional state of a randomly selected individual at timestep t.cos 2π is a stochastic vector following a uniform distribution [37].

C. Lévy flight

In spectral optimization algorithms, stochastic parameters determine the step size adjustments during both the global and local exploration phases. Although the underlying random variables are typically uniformly distributed, traditional mechanisms often lack sufficient directional bias and show limited exploration efficiency. To address these issues, this study introduces the Lévy flight mechanism [12] to enhance the global search capability of the original LSO, thereby mitigating premature convergence to suboptimal regions while maintaining the balance between exploration and exploitation. Lévy flight is a stochastic motion paradigm that mimics non-Gaussian step patterns observed in random walks. Its characteristic step length follows a Lévy stable distribution, which can be mathematically described by Fourier transform analysis as:

$$F(k) = \exp\left(-\alpha |k|^{\beta}\right) \tag{20}$$

Where $\alpha \in [-1,1]$ denotes the Lévy distribution's skewness parameter. Studies confirm that the variation in β critically influences step length characteristics in Lévy flights [39]: higher β induces shorter step lengths in random walks, whereas lower β produces extended step lengths. The step length profile is mathematically defined in Equation (21):

$$S = \frac{u}{|v|^{\frac{1}{\beta}}} \tag{21}$$

Where parameters u and v are generated through Gaussian distributions defined in Equation (22), while parameter σ is specified by the formulation in Equation (23):

$$u \sim N(0, \sigma^2), v \sim N(0, \sigma^2) \tag{22}$$

$$\sigma = \left[\frac{\Gamma(1+\beta)\sin\left(\frac{\pi\beta}{2}\right)}{\Gamma\left(\frac{1+\beta}{2}\right)\beta \times 2^{\frac{\beta-1}{2}}} \right]^{\frac{1}{\beta} \times (0.5 - rand)} \tag{23}$$

Where Γ denotes the Euler-Mascheroni gamma function, and rand represents a uniformly distributed random variable in [0,1]. Referencing related literature, the optimal range for the parameter β is [1, 2], and in this paper, the value is set to 1.5 [38].

D. ELSO algorithmic framework

Building upon the above framework, the enhanced LSO integrates three optimization mechanisms: Logistic chaotic mapping-based initialization, Cauchy mutation, and Lévy flight dynamics. The algorithmic workflow is as follows:

Step 1: Initialize system parameters, including the maximum fitness value, global optimum, boundary constraint parameters, and refractive index coefficients. Step 2: Generate the initial candidate solutions using Logistic chaotic mapping-based initialization, with each solution vector corresponding to a search ray. Step 3: Evaluate the fitness of all candidate solutions and update the global optimum through competitive comparison. Step 4: Apply Cauchy mutation, guided by the current global optimum position and with dynamically modulated probability (see Equation 8), then execute Step 3. Step 5: Adjust the search direction vectors using Lévy flight trajectories (see Equation 9), and balance exploration and exploitation through information sharing within the population. Step 6: Select better solutions from the candidate pool based on their fitness values, then update the next set of candidate solutions. Step 7: Repeat Steps 4–6 until the convergence condition is met. Step 8: Output the optimized solution vector and terminate the algorithm.

Fig.2 visually formalizes the ELSO algorithmic architecture, with the complete workflow diagram presented in the figure caption.

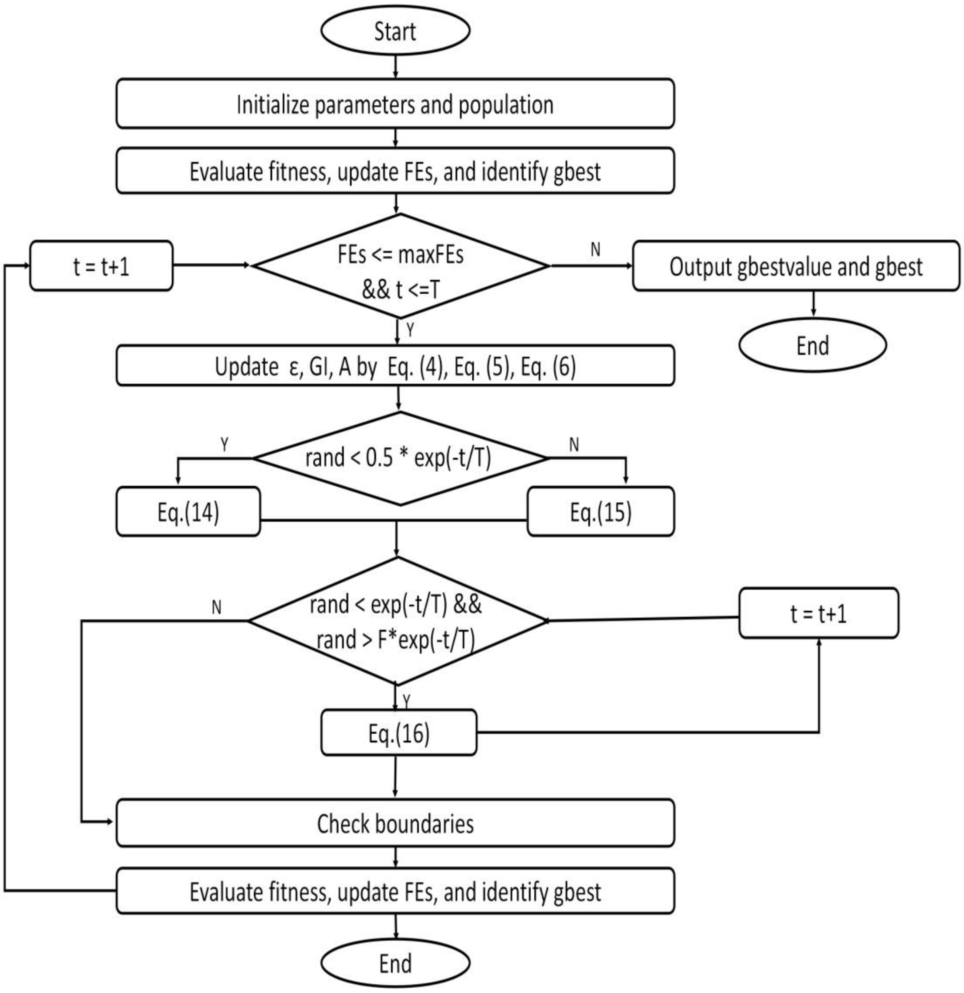

Fig. 2 Flow chart of the ELSO

IV. Benchmark funcitons and parameter settings

A. Benchmark Function Evaluation

The performance of the proposed ELSO algorithm was systematically evaluated using the CEC2017 benchmark suite, which is a comprehensive set of test problems. This suite encompasses four categories of functions: unimodal, multimodal, hybrid, and composite.

B. Parameter Configuration

Table II compares the proposed ELSO algorithm with other algorithms using standardized parameter settings adopted from the literature. The selected benchmark algorithms encompass a variety of optimization paradigms and have demonstrated effective global search capabilities.

C. Experimental results and data analysis

In this section, we comprehensively evaluate the performance of the ELSO algorithm. We compare the ELSO algorithm with the other algorithms listed in Table II, using the CEC2017 test suite as the benchmark. This study examines the effectiveness of the ELSO algorithm's strategies and its sensitivity to parameter settings. The application of these statistical methods aims to provide detailed and objective evidence for accurately assessing the practical performance and potential advantages of ELSO in solving various optimization problems.

D. Strategy validity analysis

The strategy effectiveness analysis confirms the validity of the enhancement strategies proposed in this study. To evaluate the improvements in LSO algorithm performance resulting from individual and combined enhancement strategies, three core components were designed: Logistic chaotic mapping, Cauchy mutation, and Lévy Flight [21]. By progressively integrating these three strategies into the LSO framework, the ELSO algorithm was ultimately developed, achieving an optimal balance between exploration and exploitation through an innovative initialization method and an adaptive search mechanism that incorporates all three enhancements. Experimental results demonstrate that the synergistic application of these strategies leads to statistically significant performance improvements, outperforming the use of any single component.

As demonstrated in Fig. 3, each intermediate algorithm was independently executed 30 times under identical parameter configurations. Convergence performance improves progressively across algorithm iterations, from LSO to intermediate variants and finally to ELSO. This trend confirms the cumulative effectiveness of the enhancement strategies.

Statistical analysis shows ELSO is significantly superior ($p<0.05$) to baseline LSO and intermediate variants, validating the effectiveness of the proposed enhancement framework.

E. Parameter sensitivity analysis

Parameter selection plays a crucial role in the performance of algorithms and represents an essential component of system optimization. Sensitivity analysis systematically identifies the key parameters that significantly affect performance. This enables targeted parameter tuning and improves optimization outcomes. The ELSO algorithm involves two adjustable parameters: α (the regulation parameter), which controls the balance between exploration and exploitation during the search process, and β (the adaptive update probability), which determines the probability of moving a solution toward the optimal region. These parameters strongly influence how the algorithm behaves. Therefore, systematic sensitivity analysis is essential to identify their optimal settings. Therefore, we conducted a sensitivity analysis based on the CEC 2017 benchmark function set to quantitatively evaluate the impact of each parameter on the algorithm's performance. Parameter selection plays a crucial role in the performance of algorithms and represents an essential component of system optimization. Sensitivity analysis systematically identifies the key parameters that significantly affect performance. This enables targeted parameter tuning and improves optimization outcomes. The ELSO algorithm involves two adjustable parameters: α (the regulation parameter), which controls the balance between exploration and exploitation during the search process, and β (the adaptive update probability), which determines the probability of moving a solution toward the optimal region. These parameters strongly influence how the algorithm behaves. Therefore, systematic sensitivity analysis is essential to identify their optimal settings. Therefore, we conducted a sensitivity analysis based on the CEC 2017 benchmark function set to quantitatively evaluate the impact of each parameter on the algorithm's performance.

Preliminary experimental results show that ELSO performs reliably when $\alpha \in [0.1,1.0]$ and $\beta \in [0.2,2.0]$. To determine the optimal parameter settings, we conducted a systematic grid search analysis as part of our methodology.

Specifically, in order to achieve an optimal balance between solution accuracy and computational efficiency, a 10×10 uniformly spaced grid was constructed across these parameter intervals (α: 0.1-1.0 with 0.1 increments; β: 0.2-2.0 with 0.2 increments), resulting in a total of 100 parameter combinations [22].

The parameters of the ELSO algorithm were set as follows: the population size N was 50, the maximum number of function evaluations was 1.0×10^5, and the maximum number of iterations T was 2000. For each parameter configuration, thirty independent runs were performed. The results are visualized in Fig. 4. The heatmap in Fig. 4 shows ELSO's performance rankings for each parameter combination, based on the mean optimization metrics from the CEC2017 benchmark set.

Fig.4 shows that the ELSO algorithm attains its optimal

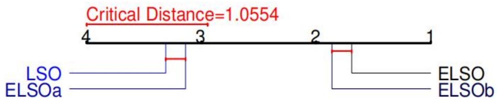

Fig. 3 Strategy effectiveness analysis diagram

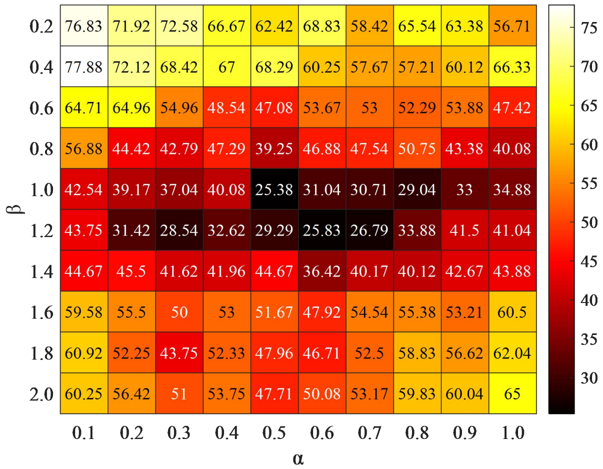

Fig. 4 Parameter sensitivity analysis diagram

performance when α=0.5 and β=1. Although this parameter combination may not be theoretically optimal, it demonstrated statistically significant superiority (p<0.05) compared to the 100 configurations evaluated. Therefore, we selected α=0.5 and β=1 as the parameters for ELSO. These values were used in all the following experiments.

V. EXPERIMENTS AND COMPARATIVE ANALYSIS

A. Qualitative comparison between LSO and ELSO

This study conducts a qualitative comparison between LSO and ELSO from key algorithmic perspectives, including search history plots, population diversity, and the balance between exploration and exploitation. Focusing on functional attributes, the analysis employs two CEC2017 benchmark functions: f_1 and f_6. Function f_1 is unimodal, featuring a smooth topology with a single global optimum. In contrast, f_6 is multimodal and exhibits complex, multi-peaked structures with distributed sub-optimal regions. This dual-function evaluation framework enables a systematic comparison of algorithm performance in both simple optimization scenarios, as represented by f_1, and complex fitness landscapes, as represented by f_6.

To enhance the visualization of results, the dimensionality of both f_1 and f_6 is set to 2. In the experiments, the parameter settings for LSO and ELSO are as follows: population size N=20, maximum iterations T=500, and maximum fitness evaluations FEs=1×10^4.

As shown in Figs. 5 and 6, the search history plots systematically divide the evolutionary process of the algorithms into four distinct temporal phases (PI–PIV). The progression from PI to PIV reveals that the population distribution of ELSO gradually shifts from a dispersed spatial pattern to a clustered configuration, whereas LSO maintains spatial dispersion throughout all iteration phases. This comparative visualization quantitatively highlights the improved convergence efficiency of ELSO and the persistent exploration tendency of LSO.

The population diversity dynamics presented in Figs. 5 and 6 indicate that ELSO experiences a rapid decrease in diversity during the initial phases (PI–PII), demonstrating accelerated convergence and higher global search efficiency. In contrast, LSO exhibits relatively stable diversity throughout the iterative process, reflecting insufficient convergence performance. Further analysis of the later stages (PIII–PIV) reveals that ELSO's diversity stabilizes near the optimal region (as the variance approaches zero), while LSO continues to fluctuate, which hinders the aggregation of effective solutions. The comparative exploration-exploitation ratios further quantitatively confirm that ELSO demonstrates superior switching ability between these two processes, achieving rapid exploration in the early phases and precise exploitation in the later stages.

In summary, a comprehensive analysis of search trajectory patterns and exploration-exploitation ratios confirms that ELSO has higher convergence efficiency and more robust optimization performance.

B. Quantitative analysis with other algorithms

To further confirm the superior performance of ELSO, we conducted both the Wilcoxon rank-sum test and the Friedman test. The Wilcoxon rank-sum test, which is based on the ranking of data, effectively reduces the influence of outliers on the results. In contrast, the Friedman test is a non-parametric method used to compare differences among three or more related samples, making it suitable for analyzing repeated measures data. This test is effective in identifying differences among multiple treatment groups, which is essential for comparing the performance of several algorithms. Together, these two statistical approaches both address common data variability in empirical studies and provide a rigorous analytical foundation for algorithm performance comparison, thus enhancing the reliability of research conclusions.

These two statistical methodologies not only effectively address common data variability in empirical research but also establish rigorous analytical foundations for algorithm performance comparison, thereby enhancing the reliability of research conclusions.

In this study, ELSO and the comparative algorithms (listed in Table II) were configured according to established methodological guidelines. All comparison algorithms used a population size of N=50, a maximum of 1.0×10^5 evaluations, and were independently run 30 times to ensure the reliability of the results. The experiments included both 30-dimensional and 50-dimensional benchmark functions from the CEC2017 test suite, and the comparative results are systematically presented. Tables III and IV report performance metrics as follows: the "*Rank*" columns indicate the ranking of algorithms based on ascending performance values; the "*Mean*" columns show mean performance metrics sorted by average performance; "*Overall Rank*" aggregates individual rankings across all functions; and "*Final Rank*" is determined by summing the "*Overall Rank*" values.

The data in Tables III and IV clearly show that the ELSO algorithm ranks first in both the 30-dimensional and 50-dimensional test functions, indicating that ELSO outperforms the comparison algorithms in terms of overall performance.

In addition, the "*total ranking*" value of ELSO is significantly lower than those of the competing algorithms, further confirming its superior performance. The "*mean*" metric provides a comprehensive evaluation of the algorithm's effectiveness: In 30 dimensions, ELSO achieves 14 best results and 11 second-best results, in 50 dimensions, it achieves 15 best results and no worst results.

By contrast, the second-best algorithm in 30 dimensions only achieves 3 best and 10 second-best results, while HCLPSO, the second-best in 50 dimensions, obtains 6 best and 8 second-best results. Thus, ELSO demonstrates clear superiority over the other algorithms. The "Std" metric is used to assess the stability of the algorithms: ELSO achieves 14 best and 11 second-best results in 30 dimensions, and 14 best and 10 second-best results in 50 dimensions, without any worst results. Consequently, ELSO's stability is noticeably better than that of the other algorithms. Fig. 7 presents the Friedman test results for the "mean," "standard deviation," and "best" metrics.

C. Wilcoxon signed-rank test

The Wilcoxon signed-rank test was performed with a significance level of $\alpha = 0.05$. Table V presents a summary of the comparative evaluation results. The statistical notations are defined as follows: R^+ represents the sum of positive ranks, indicating instances where ELSO outperforms the benchmark algorithms; R^- denotes the sum

TABLE II. PARAMETER SETTINGS OF THE COMPARED ALGORITHMS

No.	Algorithm	Parameters settings	Year	Reference
1	ASO	$\alpha = 50, \beta = 0.2$	2019	[13]
2	HGworf	$a = 2 - t * ((2)/T), \beta = 1.5$	2023	[14]
3	AHA	Inertia weight $w = 0.4\sim0.9$, $c_1 = 2.0$, $c_2 = 2.0$	2022	[15]
4	HBA	$\alpha = 0.5\sim2.0$, $\beta = 0.5\sim2.0$, Memory Update Probability p = 0.8~0.95	2022	[16]
5	TS	Tabu List Size $T = 0.1\sim0.2$	2022	[17]
6	LSO	$\alpha = 0.5, \beta = 0.2$	2021	[18]
7	HCLPSO	Inertia weight $w = 0.2\sim0.99$, $c = 1.5$	2021	[19]
8	SO	Threshold(*food*) = 0.25, Threshold(*temp*) = 0.25	2022	[20]
9	ELSO	$\alpha = 0.5, \beta = 1$	Present	Present

negative ranks, reflecting cases where ELSO underperforms. The symbol "+" indicates that ELSO exhibits statistically significant superiority on the majority of test functions, "-" denotes the opposite outcome, and "=" represents no statistically significant difference in performance.

The experimental results reported in Table V demonstrate that ELSO achieves superior comparative performance across 21 benchmark functions ($f_1, f_3, f_4, f_5, f_7, f_8, f_{11}, f_{12}, f_{14}, f_{15}, f_{17}, f_{18}, f_{19}, f_{20}, f_{21}, f_{23}, f_{24}, f_{25}, f_{26}, f_{27}, f_{28}, f_{29}, f_{30}$). This is evidenced by statistically significant p-values, substantially higher R^+ values, and consistently low R^- values. Under the statistical significance criterion (h=1), these findings further substantiate the consistent and significant superiority of ELSO over the comparative algorithms in terms of overall performance.

D. Convergence curve comparison

The convergence curves intuitively illustrate the trajectories of various optimization algorithms as they progressively approach the optimal solution across multiple iterative processes. By meticulously analyzing these curves, the performance of different algorithms can be quantitatively and objectively evaluated, allowing researchers to clearly identify which methods achieve the target with faster convergence speed or higher solution accuracy under diverse experimental conditions. To systematically investigate optimization dynamics in different scenarios, this study selected 30 benchmark functions with diverse characteristics and dimensionalities, ensuring broad representativeness and stability. The detailed convergence progress of these functions is visually depicted in Fig. 8.

The results indicate that ELSO achieves a rapid reduction in the fitness function value during the initial iterations, demonstrating effective exploration of promising solution regions and accelerated optimization enabled by adaptive search mechanisms. Further comparative analysis shows that ELSO achieves a smoother descent during the early stages of convergence. This makes it more effective than other algorithms at avoiding local optima. In the subsequent iterations, ELSO exhibits minimal fluctuations in fitness values, thereby confirming its strong convergence stability after finding the optimal solution. Although ELSO's early convergence speed is similar to that of comparative algorithms for some benchmark functions, its optimization speed improves significantly in the later stages of iteration. The final convergence results show that ELSO consistently achieves better solution accuracy on most test functions, further verifying that the synergistic enhancement mechanism substantially improves both the convergence stability and adaptability of the algorithm.

VI. Performance validation of the ELSO algorithm on typical engineering optimization problems

Engineering optimization problems provide an effective means for evaluating the real-world performance of the ELSO algorithm. In this section, four representative engineering optimization problems are selected for a further assessment of ELSO's effectiveness. The experimental suite encompasses four classical engineering optimization problems: the spring design problem, the reducer design problem, the wireless sensor network (WSN) coverage optimization problem, and the bridge arch design optimization problem. Among these, the WSN coverage optimization and bridge arch design problems are classified as unconstrained optimization problems, while the spring design and reducer design problems are considered constrained optimization problems. To enhance ELSO's capability in addressing constrained optimization challenges, the FDC handling method is introduced in this study. The operational framework of this method is outlined as follows:

$$Minimize / Maximize : f(X) \tag{24}$$

$$S:\left\{\begin{array}{l} g_j(X) \le 0, j = 1, ..., p \\ h_k(X) = 0, k = p+1, ..., m \end{array}\right. \tag{25}$$

The equation above presents a generalized mathematical model for constrained optimization problems, which typically consist of decision variables, a search space, constraint functions, and an objective function. Here, S represents the decision space, X denotes the d-dimensional solution vector; $f(x)$ is the objective function; $h_k(X)$ and $g_j(X)$ correspond to the k_th equality constraint and the j_th inequality constraint, respectively, and p and m are the numbers of equality and inequality constraints.

TABLE V. Wilcoxon signed rank test results

ELSO Vs	Ranked in different dimensions					
	D=30			D=50		
	R+	R-	+/=/-	R+	R-	+/=/-
ASO	275.72	189.28	17/3/9	302.28	162.72	19/4/6
HGworf	331.21	133.79	21/3/5	319.28	145.72	19/2/8
AHA	337.21	127.79	20/7/2	391.41	73.59	26/2/1
HBA	387.07	77.93	25/2/2	416.55	48.45	26/2/1
TS	382.66	82.34	25/1/3	415.52	49.48	26/1/2
LSO	397.41	67.59	24/1/4	421.62	43.38	26/1/2
HCLPSO	261.69	203.31	15/7/7	291.14	173.86	17/3/9
SO	344.45	120.55	21/6/2	404.41	60.59	27/1/2
p-value	1.86E-02	4.94E-02	1.26E-01	3.31E-02	4.65E-03	2.32E-03

TABLE III
RESULTS OF COMPARING ALGORITHMS ON THE CEC2017 BENCHMARK FUNCTION (D=30)

$f(x)$	Index	ASO	HGWO	AHA	HBA	TS	LSO	HCLPSO	SO	ELSO
f_1	Mean	2.0843E+03	4.5194E+03	3.9819E+03	5.5849E+03	1.2440E+06	2.0180E+03	2.1692E+03	7.9722E+03	1.0456E+02
	Std	2.2188E+03	6.5798E+03	4.7627E+03	5.8642E+03	3.6609E+05	1.4776E+03	2.4957E+03	1.2984E+04	8.4531E+00
	Best	1.0747E+02	1.0077E+02	1.7464E+02	1.1188E+02	7.9250E+05	1.2969E+02	1.0201E+02	1.6952E+02	1.0000E+02
	Rank	3	6	5	7	9	2	4	8	1
f_3	Mean	1.8663E+04	3.2370E+02	4.8373E+03	2.7872E+04	3.2852E+04	2.2120E+03	1.1586E+03	3.9708E+04	1.8907E+03
	Std	8.6352E+03	3.8347E+01	2.0479E+03	7.0168E+03	3.9069E+03	9.1816E+02	9.8739E+02	1.0472E+04	1.3571E+03
	Best	7.9378E+03	3.0005E+02	1.4349E+03	1.9918E+04	2.3157E+04	6.5860E+02	3.3527E+02	1.7989E+04	5.2032E+02
	Rank	6	1	5	7	8	4	2	9	3
f_4	Mean	5.2266E+02	5.0189E+02	4.9591E+02	4.8692E+02	4.9268E+02	4.8707E+02	5.0166E+02	4.9296E+02	4.8817E+02
	Std	2.0818E+01	4.3961E+01	2.6330E+01	1.3408E+01	1.6532E+01	2.5486E+01	1.6802E+01	1.7896E+01	2.4821E+01
	Best	4.6518E+02	4.0000E+02	4.6427E+02	4.6414E+02	4.7114E+02	4.0659E+02	4.6915E+02	4.6806E+02	4.0003E+02
	Rank	9	8	6	1	4	2	7	5	3
f_5	Mean	5.3937E+02	5.4464E+02	6.3585E+02	6.1882E+02	6.4660E+02	5.7745E+02	5.4272E+02	5.5884E+02	5.4053E+02
	Std	1.0132E+01	1.2853E+01	3.6464E+01	2.1302E+01	2.1717E+01	1.2570E+01	1.3387E+01	9.8073E+00	8.1752E+00
	Best	5.2388E+02	5.2686E+02	5.7164E+02	5.6766E+02	6.1190E+02	5.4673E+02	5.2686E+02	5.3487E+02	5.2587E+02
	Rank	1	4	8	7	9	6	3	5	2
f_6	Mean	6.0005E+02	6.0790E+02	6.0375E+02	6.0189E+02	6.0789E+02	6.0001E+02	6.0000E+02	6.0163E+02	6.0000E+02
	Std	1.1368E-01	2.3257E+00	6.8084E+00	3.9351E+00	2.7966E+00	1.9535E-03	4.5130E-05	1.0574E+00	3.1986E-03
	Best	6.0000E+02	6.0462E+02	6.0005E+02	6.0002E+02	6.0369E+02	6.0000E+02	6.0000E+02	6.0018E+02	6.0000E+02
	Rank	4	9	7	6	8	3	1	5	2
f_7	Mean	7.5427E+02	7.8570E+02	9.5108E+02	8.5985E+02	8.8785E+02	8.1497E+02	7.9511E+02	8.2062E+02	7.7349E+02
	Std	6.5382E+00	1.7539E+01	6.4541E+01	5.6046E+01	2.8501E+01	1.2397E+01	1.3662E+01	3.4302E+01	1.1510E+01
	Best	7.4670E+02	7.6573E+02	8.1847E+02	7.9407E+02	8.3639E+02	7.9873E+02	7.6257E+02	7.7570E+02	7.5621E+02
	Rank	1	3	9	7	8	5	4	6	2
f_8	Mean	8.3754E+02	8.3804E+02	9.1601E+02	8.8316E+02	9.1382E+02	8.7734E+02	8.5234E+02	8.5988E+02	8.4274E+02
	Std	7.5545E+00	1.1684E+01	2.1107E+01	1.3651E+01	1.5389E+01	1.3579E+01	1.4174E+01	1.1932E+01	1.1071E+01
	Best	8.1592E+02	8.2487E+02	8.8358E+02	8.5672E+02	8.7948E+02	8.5387E+02	8.3184E+02	8.4002E+02	8.2487E+02
	Rank	1	2	9	7	8	6	4	5	3
f_9	Mean	9.0000E+02	1.1445E+03	3.1875E+03	2.6381E+03	4.0998E+03	1.1782E+03	9.2514E+02	1.1128E+03	9.0063E+02
	Std	4.7206E-14	1.0923E+02	1.0576E+03	9.2849E+02	4.4041E+02	1.8491E+02	3.8636E+01	9.8850E+01	6.7406E-01
	Best	9.0000E+02	9.1830E+02	1.5868E+03	9.3198E+02	3.0068E+03	9.5016E+02	9.0027E+02	9.5005E+02	9.0000E+02
	Rank	1	5	8	7	9	6	3	4	2
f_{10}	Mean	4.0033E+03	4.4369E+03	4.1850E+03	5.3740E+03	4.3126E+03	4.6322E+03	4.1384E+03	3.3018E+03	3.6928E+03
	Std	6.0695E+02	6.8129E+02	5.7208E+02	1.0562E+03	4.2126E+02	2.7639E+02	5.9408E+02	4.0611E+02	6.3651E+02
	Best	2.7860E+03	3.2401E+03	3.0398E+03	3.2514E+03	3.3131E+03	3.9186E+03	2.9493E+03	2.5695E+03	2.5823E+03
	Rank	3	7	5	9	6	8	4	1	2
f_{11}	Mean	1.2002E+03	1.1995E+03	1.1803E+03	1.2125E+03	1.2114E+03	1.2000E+03	1.1653E+03	1.2223E+03	1.1312E+03
	Std	3.9342E+01	3.4106E+01	3.3299E+01	5.3604E+01	2.8918E+01	1.7711E+01	3.1111E+01	4.0884E+01	2.5002E+01
	Best	1.1507E+03	1.1528E+03	1.1316E+03	1.1415E+03	1.1680E+03	1.1563E+03	1.1272E+03	1.1494E+03	1.1074E+03
	Rank	6	4	3	8	7	5	2	9	1
f_{12}	Mean	4.3930E+05	1.6108E+05	1.0241E+06	6.2004E+05	1.3867E+06	5.1168E+03	7.6339E+04	2.9108E+05	2.5580E+04
	Std	3.7178E+05	2.9288E+05	5.8206E+05	5.7153E+05	8.5472E+05	1.2413E+03	4.3205E+04	2.2651E+05	1.4911E+04
	Best	4.4668E+04	2.8358E+04	9.8936E+04	6.5240E+04	1.7517E+05	3.3675E+03	1.4981E+04	5.3656E+04	6.8660E+03
	Rank	6	4	8	7	9	1	3	5	2
f_{13}	Mean	1.1539E+04	2.0117E+04	1.7584E+04	3.0613E+04	4.4635E+03	1.6181E+03	1.3466E+04	1.5389E+04	7.2636E+03
	Std	6.2580E+03	1.4533E+04	1.3701E+04	4.6003E+04	2.8483E+03	7.2935E+01	1.1069E+04	7.9752E+03	5.3130E+03
	Best	3.7865E+03	3.9617E+03	1.7280E+03	2.9617E+03	2.3111E+03	1.4768E+03	1.9209E+03	2.3947E+03	1.4315E+03
	Rank	4	8	7	9	2	1	5	6	3
f_{14}	Mean	1.7417E+04	4.3893E+04	1.0312E+04	1.0114E+04	2.3312E+05	1.4652E+03	1.6644E+04	8.9631E+03	1.4431E+03
	Std	2.7878E+04	1.1263E+05	9.4612E+03	6.8934E+03	2.1160E+05	7.2230E+00	8.1917E+03	8.3717E+03	9.4375E+00
	Best	1.8558E+03	1.8880E+03	1.6238E+03	3.2472E+03	1.2488E+04	1.4542E+03	2.4685E+03	1.7642E+03	1.4222E+03
	Rank	7	8	5	4	9	2	6	3	1
f_{15}	Mean	5.4649E+03	5.1093E+03	3.8947E+03	8.6807E+03	1.8335E+03	1.6039E+03	3.6413E+03	6.6222E+03	1.5562E+03
	Std	3.8321E+03	3.5602E+03	2.8508E+03	1.2955E+04	1.9250E+02	1.8818E+01	2.9516E+03	3.3137E+03	3.6958E+01
	Best	1.6447E+03	1.6357E+03	1.5800E+03	1.6739E+03	1.6057E+03	1.5761E+03	1.5331E+03	2.0266E+03	1.5097E+03
	Rank	7	6	5	9	3	2	4	8	1
f_{16}	Mean	2.4602E+03	2.2238E+03	2.6581E+03	2.5592E+03	2.5414E+03	2.5251E+03	2.2256E+03	2.2091E+03	2.0832E+03
	Std	2.8338E+02	3.0141E+02	3.2269E+02	2.3859E+02	2.1169E+02	1.6231E+02	1.7550E+02	2.4651E+02	2.1043E+02
	Best	1.7254E+03	1.7471E+03	1.9469E+03	2.2741E+03	2.1861E+03	2.2575E+03	1.8684E+03	1.8753E+03	1.7396E+03
	Rank	5	3	9	8	7	6	4	2	1

CONTINUED TABLE III

$f(x)$	Index	ASO	HGWO	AHA	HBA	TS	LSO	HCPLSO	SO	ELSO
f_{17}	Mean	1.9457E+03	1.8644E+03	2.1253E+03	2.1992E+03	2.1383E+03	1.8862E+03	1.8316E+03	2.0544E+03	1.7832E+03
	Std	1.3074E+02	9.4049E+01	1.8293E+02	2.4667E+02	1.9565E+02	6.3020E+01	1.0416E+02	1.7585E+02	7.4494E+01
	Best	1.7616E+03	1.7451E+03	1.8620E+03	1.7583E+03	1.8286E+03	1.7946E+03	1.7559E+03	1.8064E+03	1.7151E+03
	Rank	5	3	7	9	8	4	2	6	1
f_{18}	Mean	2.4731E+05	1.2872E+05	1.1377E+05	2.8935E+05	2.2548E+05	1.8873E+03	1.4690E+05	2.5448E+05	7.7632E+03
	Std	1.7211E+05	7.9159E+04	8.7295E+04	2.3786E+05	2.5661E+05	1.1921E+01	1.0297E+05	2.7019E+05	5.5023E+03
	Best	1.3424E+04	3.2713E+04	2.6611E+04	7.3909E+04	3.8189E+04	1.8671E+03	3.4674E+04	4.6917E+04	2.3812E+03
	Rank	7	4	3	9	6	1	5	8	2
f_{19}	Mean	5.6163E+03	6.0228E+03	7.3474E+03	1.1365E+04	2.9921E+03	1.9386E+03	9.1917E+03	1.0362E+04	1.9241E+03
	Std	4.1011E+03	3.9342E+03	7.1964E+03	1.3038E+04	1.0101E+03	5.7533E+00	9.2551E+03	7.7292E+03	1.4743E+01
	Best	2.0656E+03	2.0827E+03	2.1322E+03	2.1144E+03	1.9688E+03	1.9284E+03	1.9755E+03	2.2350E+03	1.9110E+03
	Rank	4	5	6	9	3	2	7	8	1
f_{20}	Mean	2.2841E+03	2.2510E+03	2.4620E+03	2.4546E+03	2.4170E+03	2.2941E+03	2.2055E+03	2.2768E+03	2.1022E+03
	Std	1.2812E+02	9.0715E+01	1.4329E+02	1.9959E+02	1.4234E+02	7.5321E+01	9.2427E+01	1.1725E+02	7.5105E+01
	Best	2.0722E+03	2.1018E+03	2.1726E+03	2.1077E+03	2.1747E+03	2.0977E+03	2.0430E+03	2.0620E+03	2.0117E+03
	Rank	5	3	9	8	7	6	2	4	1
f_{21}	Mean	2.3377E+03	2.3423E+03	2.4113E+03	2.3959E+03	2.4263E+03	2.3761E+03	2.3495E+03	2.3608E+03	2.3394E+03
	Std	1.1662E+01	1.2941E+01	3.1405E+01	3.1396E+01	5.9868E+01	1.1422E+01	1.8097E+01	1.1169E+01	1.0155E+01
	Best	2.3165E+03	2.3236E+03	2.3609E+03	2.3441E+03	2.2170E+03	2.3569E+03	2.3266E+03	2.3368E+03	2.3237E+03
	Rank	1	3	8	7	9	6	4	5	2
f_{22}	Mean	2.5284E+03	2.6400E+03	2.3008E+03	2.8802E+03	2.4612E+03	2.3068E+03	2.3001E+03	3.3572E+03	2.3002E+03
	Std	8.7497E+02	1.0504E+03	1.3629E+00	1.5413E+03	8.1086E+02	8.3931E+00	6.1394E-01	1.3342E+03	9.8439E-01
	Best	2.3000E+03	2.3000E+03	2.3000E+03	2.3000E+03	2.3100E+03	2.3000E+03	2.3000E+03	2.3000E+03	2.3000E+03
	Rank	6	7	3	8	5	4	1	9	2
f_{23}	Mean	2.7280E+03	2.7052E+03	2.7777E+03	2.7495E+03	2.8338E+03	2.7236E+03	2.7080E+03	2.7379E+03	2.6915E+03
	Std	3.0760E+01	1.7134E+01	3.1620E+01	2.9552E+01	3.6511E+01	1.2173E+01	1.5550E+01	2.0964E+01	1.0200E+01
	Best	2.6821E+03	2.6753E+03	2.7283E+03	2.7090E+03	2.7585E+03	2.7053E+03	2.6782E+03	2.7120E+03	2.6691E+03
	Rank	5	2	8	7	9	4	3	6	1
f_{24}	Mean	2.8599E+03	2.8802E+03	2.9624E+03	2.9909E+03	3.1303E+03	2.8838E+03	2.8833E+03	2.9016E+03	2.8629E+03
	Std	3.1057E+01	2.6477E+01	3.5579E+01	1.9708E+02	8.9573E+01	9.4927E+00	2.2717E+01	2.9847E+01	1.0443E+01
	Best	2.8064E+03	2.8404E+03	2.8600E+03	2.8692E+03	2.9413E+03	2.8612E+03	2.8434E+03	2.8564E+03	2.8469E+03
	Rank	1	3	7	8	9	5	4	6	2
f_{25}	Mean	2.8924E+03	2.9047E+03	2.9044E+03	2.8962E+03	2.8902E+03	2.8873E+03	2.8878E+03	2.8874E+03	2.8871E+03
	Std	9.6345E+00	1.6564E+01	1.9987E+01	1.6041E+01	5.5389E+00	3.0645E-01	8.6814E-01	1.1684E+00	1.2800E+00
	Best	2.8873E+03	2.8843E+03	2.8838E+03	2.8835E+03	2.8841E+03	2.8868E+03	2.8838E+03	2.8836E+03	2.8836E+03
	Rank	6	9	8	7	5	2	4	3	1
f_{26}	Mean	3.5627E+03	4.1831E+03	3.5298E+03	4.3776E+03	2.8612E+03	4.2493E+03	3.5363E+03	4.7776E+03	4.0728E+03
	Std	6.1683E+02	2.1130E+02	1.2958E+03	7.6752E+02	8.4496E+01	3.9806E+02	5.5220E+02	2.6138E+02	1.5532E+02
	Best	2.8000E+03	3.8019E+03	2.8001E+03	2.8001E+03	2.8229E+03	3.3248E+03	2.8000E+03	4.0949E+03	3.6576E+03
	Rank	4	6	2	8	1	7	3	9	5
f_{27}	Mean	3.2854E+03	3.2311E+03	3.2595E+03	3.4204E+03	3.2343E+03	3.2335E+03	3.2236E+03	3.2546E+03	3.2078E+03
	Std	4.7231E+01	1.2245E+01	1.9412E+01	1.7838E+02	1.3000E+01	9.8298E+00	6.1171E+00	1.2014E+01	5.2602E+00
	Best	3.2156E+03	3.2124E+03	3.2296E+03	3.2148E+03	3.2081E+03	3.2166E+03	3.2136E+03	3.2362E+03	3.1999E+03
	Rank	8	3	7	9	5	4	2	6	1
f_{28}	Mean	3.2001E+03	3.2398E+03	3.2195E+03	3.5033E+03	3.2265E+03	3.2067E+03	3.2103E+03	3.2419E+03	3.1791E+03
	Std	3.3670E+01	8.6326E+01	1.8890E+01	1.0662E+03	1.7056E+01	1.3305E+01	1.9759E+01	2.2225E+01	4.1651E+01
	Best	3.1008E+03	3.1000E+03	3.1959E+03	3.2012E+03	3.2021E+03	3.1918E+03	3.1681E+03	3.2038E+03	3.1001E+03
	Rank	2	7	5	9	6	3	4	8	1
f_{29}	Mean	3.5957E+03	3.7366E+03	3.6685E+03	4.0413E+03	3.7354E+03	3.8449E+03	3.5705E+03	3.8064E+03	3.4002E+03
	Std	1.2929E+02	1.6271E+02	1.5934E+02	4.6986E+02	1.6092E+02	1.1580E+02	1.2720E+02	1.9353E+02	9.4625E+01
	Best	3.3932E+03	3.4954E+03	3.3780E+03	3.3854E+03	3.4307E+03	3.6180E+03	3.3615E+03	3.3885E+03	3.2695E+03
	Rank	3	6	4	9	5	8	2	7	1
f_{30}	Mean	1.8275E+04	7.0697E+05	9.4221E+03	5.9859E+04	1.2722E+04	8.1893E+03	7.6703E+03	1.2797E+04	7.0117E+03
	Std	7.5586E+03	1.1149E+06	2.3377E+03	8.2924E+04	3.4352E+03	1.1327E+03	1.6411E+03	7.0181E+03	1.0308E+03
	Best	1.0816E+04	1.4413E+04	6.1870E+03	8.3670E+03	7.2179E+03	6.6825E+03	5.5506E+03	7.2391E+03	5.6786E+03
	Rank	7	9	4	8	5	3	2	6	1
Total Rank		128	148	180	218	189	118	101	172	51
Final Rank		4	5	7	9	8	3	2	6	1

TABLE IV
RESULTS OF COMPARING ALGORITHMS ON THE CEC2017 BENCHMARK FUNCTION (D=50)

$f(x)$	Index	ASO	HGWO	AHA	HBA	TS	LSO	HCLPSO	SO	ELSO
f_1	Mean	3.9208E+03	3.1252E+03	1.8058E+05	4.1980E+06	5.0415E+07	3.0489E+03	2.8633E+03	7.6125E+05	3.0207E+03
	Std	4.3047E+03	4.2415E+03	1.0925E+05	3.5133E+06	8.9464E+06	3.4749E+03	3.0264E+03	8.0384E+05	3.9389E+03
	Best	1.0000E+02	1.0017E+02	6.0443E+04	1.4940E+06	2.9385E+07	4.9304E+02	1.0813E+02	1.5556E+04	1.0511E+02
	Rank	5	4	6	8	9	3	1	7	2
f_3	Mean	8.3102E+04	1.7411E+04	3.7535E+04	1.2403E+05	1.1036E+05	3.4774E+04	2.7963E+04	1.2638E+05	2.7894E+04
	Std	1.3198E+04	4.9682E+03	8.1197E+03	1.3774E+04	1.0430E+04	1.0033E+04	8.0173E+03	1.1463E+04	9.4786E+03
	Best	4.0967E+04	9.0404E+03	2.1677E+04	8.8916E+04	9.2795E+04	1.7860E+04	1.6692E+04	1.0021E+05	1.3762E+04
	Rank	6	1	5	8	7	4	3	9	2
f_4	Mean	6.1060E+02	6.0289E+02	5.7162E+02	5.7845E+02	5.5649E+02	5.3901E+02	5.2712E+02	5.8501E+02	5.2724E+02
	Std	5.0160E+01	6.0938E+01	5.7174E+01	5.3134E+01	3.0494E+01	3.7980E+01	4.8981E+01	3.3017E+01	5.3297E+01
	Best	5.3315E+02	4.6483E+02	4.5125E+02	4.6752E+02	5.0038E+02	4.5040E+02	4.2983E+02	5.0955E+02	4.2855E+02
	Rank	9	8	5	6	4	3	1	7	2
f_5	Mean	6.0321E+02	5.9008E+02	8.2118E+02	7.3362E+02	8.0546E+02	7.1049E+02	6.1959E+02	6.3339E+02	5.8980E+02
	Std	1.9962E+01	1.5030E+01	3.2437E+01	5.3318E+01	3.0365E+01	2.1470E+01	2.2538E+01	1.4762E+01	2.0244E+01
	Best	5.5771E+02	5.7164E+02	7.4078E+02	6.4321E+02	7.3967E+02	6.6336E+02	5.8059E+02	6.0511E+02	5.5572E+02
	Rank	3	2	9	7	8	6	4	5	1
f_6	Mean	6.0045E+02	6.1689E+02	6.0700E+02	6.0830E+02	6.2684E+02	6.0020E+02	6.0003E+02	6.0569E+02	6.0005E+02
	Std	7.6368E-01	3.4276E+00	6.2282E+00	5.9887E+00	5.3309E+00	1.1548E-01	4.2425E-02	2.4926E+00	8.1626E-02
	Best	6.0000E+02	6.1117E+02	6.0059E+02	6.0125E+02	6.1597E+02	6.0006E+02	6.0001E+02	6.0257E+02	6.0000E+02
	Rank	4	8	6	7	9	3	1	5	2
f_7	Mean	8.0848E+02	9.1932E+02	1.3062E+03	1.0871E+03	1.2041E+03	1.0109E+03	9.2569E+02	8.8742E+02	8.3997E+02
	Std	1.0184E+01	4.3239E+01	1.6004E+02	9.1947E+01	4.8408E+01	4.1393E+01	3.9809E+01	3.2664E+01	2.3635E+01
	Best	7.9278E+02	8.5684E+02	1.0160E+03	9.8489E+02	1.0981E+03	9.5438E+02	8.3146E+02	8.4841E+02	7.9562E+02
	Rank	1	4	9	7	8	6	5	3	2
f_8	Mean	8.9369E+02	8.9263E+02	1.1352E+03	1.0124E+03	1.1111E+03	1.0107E+03	9.4722E+02	9.2080E+02	8.8868E+02
	Std	1.8210E+01	1.7703E+01	5.7572E+01	3.0099E+01	2.8444E+01	1.9393E+01	4.2935E+01	2.0989E+01	2.0723E+01
	Best	8.5472E+02	8.5870E+02	1.0099E+03	9.5675E+02	1.0484E+03	9.7051E+02	8.9154E+02	8.9600E+02	8.5074E+02
	Rank	3	2	9	7	8	6	5	4	1
f_9	Mean	9.0035E+02	2.5425E+03	1.0393E+04	1.1019E+04	1.5641E+04	4.3750E+03	1.4000E+03	2.0034E+03	9.2281E+02
	Std	4.3983E-01	4.8397E+02	2.0712E+03	4.4110E+03	1.6623E+03	1.2383E+03	1.0735E+03	4.6504E+02	2.5576E+01
	Best	9.0000E+02	1.6704E+03	4.7919E+03	3.2625E+03	1.2306E+04	2.2499E+03	9.7587E+02	1.2588E+03	9.0445E+02
	Rank	1	5	7	8	9	6	3	4	2
f_{10}	Mean	6.3724E+03	6.9763E+03	6.3869E+03	7.5345E+03	7.2066E+03	8.5620E+03	5.6546E+03	4.7945E+03	7.8389E+03
	Std	9.5788E+02	9.7600E+02	7.3633E+02	1.5334E+03	5.4784E+02	4.5607E+02	9.0441E+02	1.0706E+03	1.2400E+03
	Best	4.3993E+03	5.7068E+03	4.7443E+03	5.1981E+03	5.6162E+03	7.5199E+03	4.5988E+03	3.6566E+03	5.5956E+03
	Rank	3	5	4	7	6	9	2	1	8
f_{11}	Mean	1.2915E+03	1.2557E+03	1.3125E+03	1.3753E+03	1.7618E+03	1.3451E+03	1.2246E+03	1.3545E+03	1.1676E+03
	Std	7.7804E+01	3.7183E+01	1.6590E+02	7.8219E+01	1.8924E+02	3.3674E+01	3.8301E+01	5.8568E+01	2.2614E+01
	Best	1.2018E+03	1.2068E+03	1.1947E+03	1.2591E+03	1.4179E+03	1.2644E+03	1.1631E+03	1.2687E+03	1.1285E+03
	Rank	4	3	5	8	9	6	2	7	1
f_{12}	Mean	1.5743E+06	8.3259E+05	5.6860E+06	1.1358E+07	1.4762E+07	9.3787E+05	1.2226E+06	6.7048E+06	8.6202E+05
	Std	7.6031E+05	6.0259E+05	3.2800E+06	7.9163E+06	6.3965E+06	4.6559E+05	4.7198E+05	3.7168E+06	5.6504E+05
	Best	6.0631E+05	1.2694E+05	1.2739E+06	4.1383E+06	8.3076E+06	2.0497E+05	4.7244E+05	1.4692E+06	1.0467E+05
	Rank	5	1	6	8	9	3	4	7	2
f_{13}	Mean	1.2729E+04	1.0131E+04	1.1894E+04	4.0861E+04	2.5323E+04	5.2824E+03	4.9749E+03	1.6611E+04	2.9505E+03
	Std	4.2209E+03	5.8886E+03	7.5843E+03	2.8640E+04	6.0738E+03	7.1225E+02	5.6872E+03	1.0242E+04	2.6232E+03
	Best	6.3974E+03	3.3457E+03	2.7681E+03	5.6993E+03	1.4680E+04	3.6734E+03	1.4188E+03	5.4736E+03	1.3715E+03
	Rank	6	4	5	9	8	3	2	7	1
f_{14}	Mean	1.1962E+05	4.7394E+04	8.1719E+04	2.5581E+05	9.4108E+05	1.5938E+03	3.6712E+04	9.4897E+04	2.3972E+03
	Std	2.4946E+05	3.2679E+04	6.6173E+04	3.8372E+05	7.3616E+05	1.7716E+01	3.3268E+04	6.3214E+04	1.4973E+03
	Best	1.3440E+04	1.7545E+03	6.1210E+03	1.1763E+04	2.0905E+05	1.5593E+03	6.1595E+03	2.7978E+04	1.5046E+03
	Rank	7	4	5	8	9	1	3	6	2
f_{15}	Mean	3.6144E+03	8.3755E+03	1.1249E+04	1.9181E+04	6.6901E+03	2.0617E+03	6.9734E+03	1.3539E+04	5.8736E+03
	Std	1.9010E+03	4.8129E+03	6.5726E+03	8.6889E+03	3.7268E+03	8.9932E+01	3.0115E+03	6.7128E+03	3.1278E+03
	Best	1.9622E+03	1.8906E+03	2.2119E+03	4.9685E+03	2.7363E+03	1.9034E+03	2.0518E+03	3.9484E+03	1.6066E+03
	Rank	2	6	7	9	4	1	5	8	3
f_{16}	Mean	2.7396E+03	2.8079E+03	3.4176E+03	3.2433E+03	3.1416E+03	3.3239E+03	2.9467E+03	2.9446E+03	2.7149E+03
	Std	3.5875E+02	2.9839E+02	4.2891E+02	6.9149E+02	3.3101E+02	2.6236E+02	3.1332E+02	3.2284E+02	3.0591E+02
	Best	2.1556E+03	2.3688E+03	2.8247E+03	2.4455E+03	2.5502E+03	2.7308E+03	2.3692E+03	2.2724E+03	1.8626E+03
	Rank	2	3	9	7	6	8	5	4	1

CONTINUED TABLE IV

$f(x)$	Index	ASO	HGWO	AHA	HBA	TS	LSO	HCLPSO	SO	ELSO
f_{17}	Mean	2.6375E+03	2.8136E+03	3.1486E+03	2.8830E+03	3.0931E+03	2.8815E+03	2.7530E+03	2.7870E+03	2.3447E+03
	Std	2.6301E+02	2.5665E+02	2.5866E+02	2.9367E+02	2.8365E+02	1.7536E+02	2.7672E+02	2.8424E+02	1.8965E+02
	Best	2.2032E+03	2.3703E+03	2.7958E+03	2.4559E+03	2.5203E+03	2.4740E+03	2.1638E+03	2.3823E+03	1.8925E+03
	Rank	2	5	9	7	8	6	3	4	1
f_{18}	Mean	7.9641E+05	2.9747E+05	9.7419E+05	2.3789E+06	2.0465E+06	2.7128E+03	3.4963E+05	1.6981E+06	9.0386E+04
	Std	8.1511E+05	1.7785E+05	7.7553E+05	1.6717E+06	9.9747E+05	3.7420E+02	2.2517E+05	1.5375E+06	7.2172E+04
	Best	1.4030E+05	7.5718E+04	6.6677E+04	3.8036E+05	2.2893E+05	2.3383E+03	7.1722E+04	1.9212E+05	2.5654E+04
	Rank	5	3	6	9	8	1	4	7	2
f_{19}	Mean	1.4218E+04	1.9923E+04	2.2347E+04	2.1073E+04	1.1122E+04	2.0266E+03	1.0423E+04	1.4023E+04	1.5308E+04
	Std	6.0389E+03	1.0077E+04	1.0365E+04	1.0698E+04	4.1667E+03	1.7561E+01	9.1203E+03	1.2806E+04	6.7533E+03
	Best	6.1248E+03	3.4255E+03	3.4410E+03	2.6197E+03	5.0292E+03	1.9981E+03	1.9663E+03	2.4195E+03	3.2401E+03
	Rank	5	7	9	8	3	1	2	4	6
f_{20}	Mean	2.8053E+03	2.7679E+03	3.2096E+03	2.9397E+03	3.0144E+03	2.9960E+03	2.9178E+03	2.7818E+03	2.4757E+03
	Std	3.2939E+02	3.1439E+02	3.0351E+02	2.5835E+02	2.3474E+02	1.7364E+02	2.0415E+02	2.7139E+02	1.6785E+02
	Best	2.4907E+03	2.1886E+03	2.7715E+03	2.5496E+03	2.2798E+03	2.6104E+03	2.4795E+03	2.4002E+03	2.0821E+03
	Rank	4	2	9	6	8	7	5	3	1
f_{21}	Mean	2.3952E+03	2.3896E+03	2.5173E+03	2.4862E+03	2.6068E+03	2.5070E+03	2.4168E+03	2.4267E+03	2.3912E+03
	Std	2.3634E+01	2.7802E+01	3.9145E+01	4.2969E+01	3.6515E+01	2.2171E+01	2.5464E+01	1.8860E+01	1.6077E+01
	Best	2.3641E+03	2.3423E+03	2.4658E+03	2.4248E+03	2.5405E+03	2.4545E+03	2.3640E+03	2.3884E+03	2.3582E+03
	Rank	3	1	8	6	9	7	4	5	2
f_{22}	Mean	8.0725E+03	8.7956E+03	7.7620E+03	1.0132E+04	8.8813E+03	1.0361E+04	7.2705E+03	7.1474E+03	8.4564E+03
	Std	1.8462E+03	8.1693E+02	2.4650E+03	1.9450E+03	1.8581E+03	4.6547E+02	2.2835E+03	2.5233E+03	2.0599E+03
	Best	2.3000E+03	6.8961E+03	2.3016E+03	2.3254E+03	2.3527E+03	9.3514E+03	2.3000E+03	5.4494E+03	2.3000E+03
	Rank	4	6	3	8	7	9	2	1	5
f_{23}	Mean	2.9843E+03	2.8435E+03	3.0326E+03	2.9453E+03	3.1644E+03	2.9431E+03	2.8498E+03	2.9226E+03	2.8212E+03
	Std	6.4958E+01	3.2375E+01	4.2947E+01	5.5826E+01	9.0251E+01	2.7763E+01	4.8214E+01	4.2370E+01	1.9219E+01
	Best	2.8829E+03	2.7844E+03	2.9388E+03	2.8308E+03	3.0274E+03	2.8786E+03	2.8073E+03	2.8752E+03	2.7831E+03
	Rank	7	2	8	6	9	5	3	4	1
f_{24}	Mean	3.3312E+03	3.0470E+03	3.2753E+03	3.4380E+03	3.5419E+03	3.0802E+03	3.0700E+03	3.0623E+03	2.9883E+03
	Std	3.0040E+03	2.9619E+03	3.1689E+03	3.0370E+03	3.3065E+03	3.0360E+03	3.0078E+03	3.0342E+03	2.9523E+03
	Best	2.8600E+03	2.8404E+03	2.8069E+03	2.8692E+03	2.9413E+03	2.8612E+03	2.8434E+03	2.8564E+03	2.8464E+03
	Rank	7	3	2	8	9	5	4	6	1
f_{25}	Mean	3.1378E+03	3.1852E+03	3.1019E+03	3.1051E+03	3.1096E+03	3.0820E+03	3.0588E+03	3.0720E+03	3.0493E+03
	Std	3.6623E+01	6.4643E+01	2.9733E+01	3.4038E+01	1.5177E+01	2.5226E+01	2.5721E+01	2.6062E+01	2.6810E+01
	Best	3.0574E+03	3.0916E+03	3.0491E+03	3.0370E+03	3.0841E+03	3.0368E+03	2.9666E+03	2.9965E+03	2.9658E+03
	Rank	8	9	5	6	7	4	2	3	1
f_{26}	Mean	4.6377E+03	5.1705E+03	4.8854E+03	6.0634E+03	3.1785E+03	5.9822E+03	4.3717E+03	6.0798E+03	4.6797E+03
	Std	1.2922E+03	3.8470E+02	2.6487E+03	1.1844E+03	8.4885E+01	3.0456E+02	1.1199E+03	3.7576E+02	2.5236E+02
	Best	2.9000E+03	4.5986E+03	2.9069E+03	3.3640E+03	3.0339E+03	5.3435E+03	2.9002E+03	5.4984E+03	4.1933E+03
	Rank	3	6	5	8	1	7	2	9	4
f_{27}	Mean	3.8845E+03	3.4848E+03	3.6220E+03	4.0186E+03	3.5102E+03	3.5647E+03	3.4499E+03	3.6067E+03	3.2996E+03
	Std	3.2804E+02	7.2461E+01	1.3409E+02	5.0302E+02	7.4614E+01	6.8543E+01	8.0967E+01	7.4884E+01	5.1074E+01
	Best	3.4478E+03	3.3701E+03	3.3591E+03	3.3154E+03	3.3978E+03	3.4063E+03	3.3041E+03	3.4367E+03	3.2416E+03
	Rank	8	3	7	9	4	5	2	6	1
f_{28}	Mean	3.3645E+03	3.3930E+03	3.3794E+03	3.6791E+03	3.3665E+03	3.3701E+03	3.3331E+03	3.3388E+03	3.3138E+03
	Std	5.5503E+01	5.1039E+01	3.9363E+01	1.7663E+03	2.4092E+01	3.0419E+01	4.8019E+01	2.1222E+01	1.6513E+01
	Best	3.2747E+03	3.3175E+03	3.2977E+03	3.3197E+03	3.3125E+03	3.3158E+03	3.2648E+03	3.3087E+03	3.2803E+03
	Rank	4	8	7	9	5	6	2	3	1
f_{29}	Mean	3.9342E+03	4.4635E+03	4.2538E+03	5.6484E+03	4.3180E+03	4.7844E+03	3.7597E+03	4.1963E+03	3.5997E+03
	Std	2.8846E+02	3.5437E+02	2.9297E+02	1.6705E+03	2.5138E+02	2.5505E+02	1.7570E+02	2.8203E+02	2.4596E+02
	Best	3.5044E+03	3.8078E+03	3.7461E+03	3.5598E+03	3.7641E+03	4.3131E+03	3.4688E+03	3.8807E+03	3.2751E+03
	Rank	3	7	5	9	6	8	2	4	1
f_{30}	Mean	7.0596E+06	5.2828E+07	9.5014E+05	2.0732E+06	1.4935E+06	6.1387E+06	9.5172E+05	1.3973E+06	8.7342E+05
	Std	2.1370E+06	2.1816E+07	1.1957E+05	9.5770E+05	2.4060E+05	1.4149E+06	8.4434E+04	5.7968E+05	1.3018E+05
	Best	4.3966E+06	2.0387E+07	7.6776E+05	9.0186E+05	1.0028E+06	3.2263E+06	7.9965E+05	8.0341E+05	7.1401E+05
	Rank	8	9	2	6	5	7	3	4	1
Total Rank		132	130	186	219	202	146	86	144	60
Final Rank		4	3	7	9	8	6	2	5	1
f_{17}	Mean	2.6375E+03	2.8136E+03	3.1486E+03	2.8830E+03	3.0931E+03	2.8815E+03	2.7530E+03	2.7870E+03	2.3447E+03
	Std	2.6301E+02	2.5665E+02	2.5866E+02	2.9367E+02	2.8365E+02	1.7536E+02	2.7672E+02	2.8424E+02	1.8965E+02

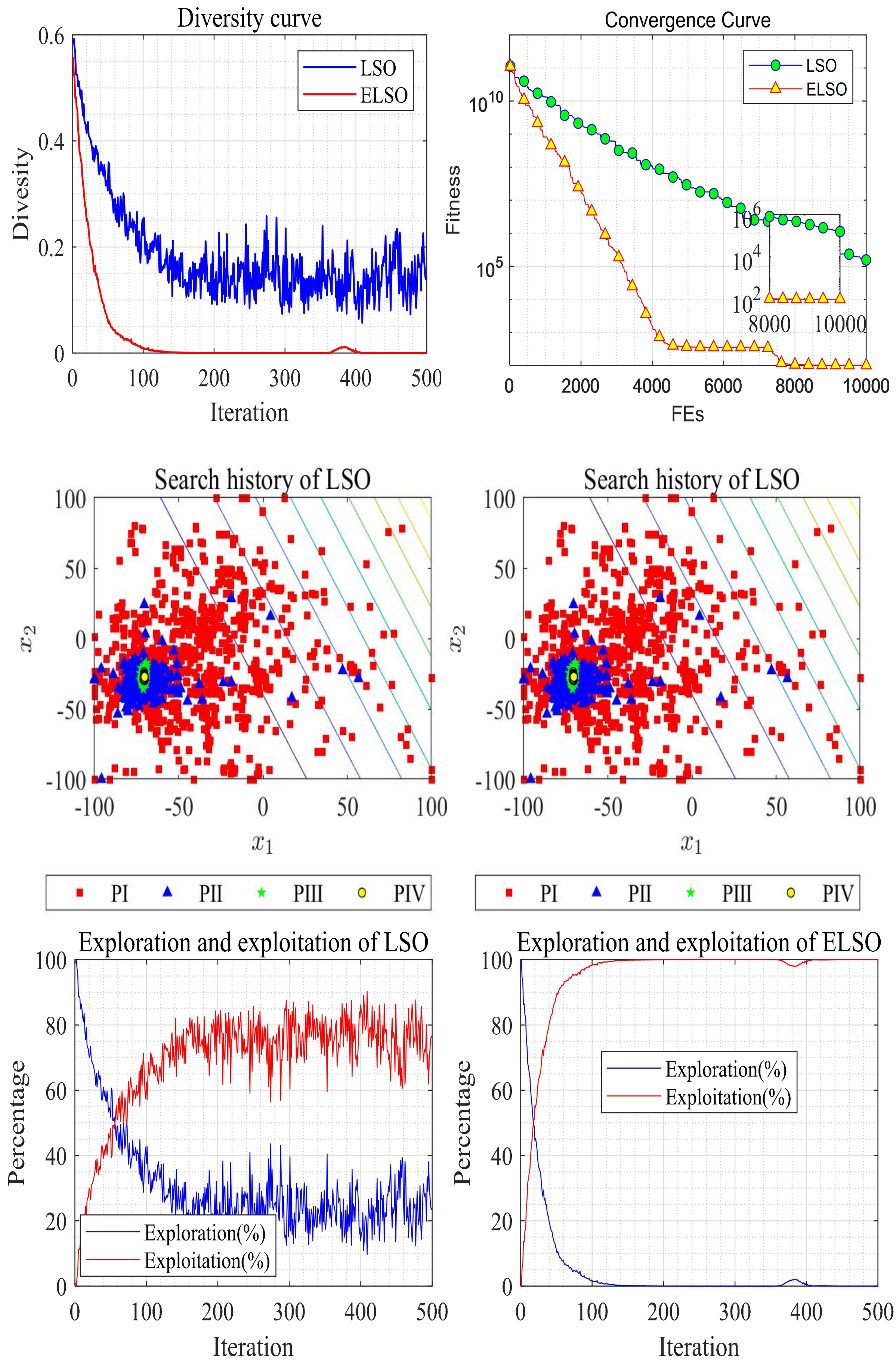

Fig. 5 Qualitative comparison results of f_1

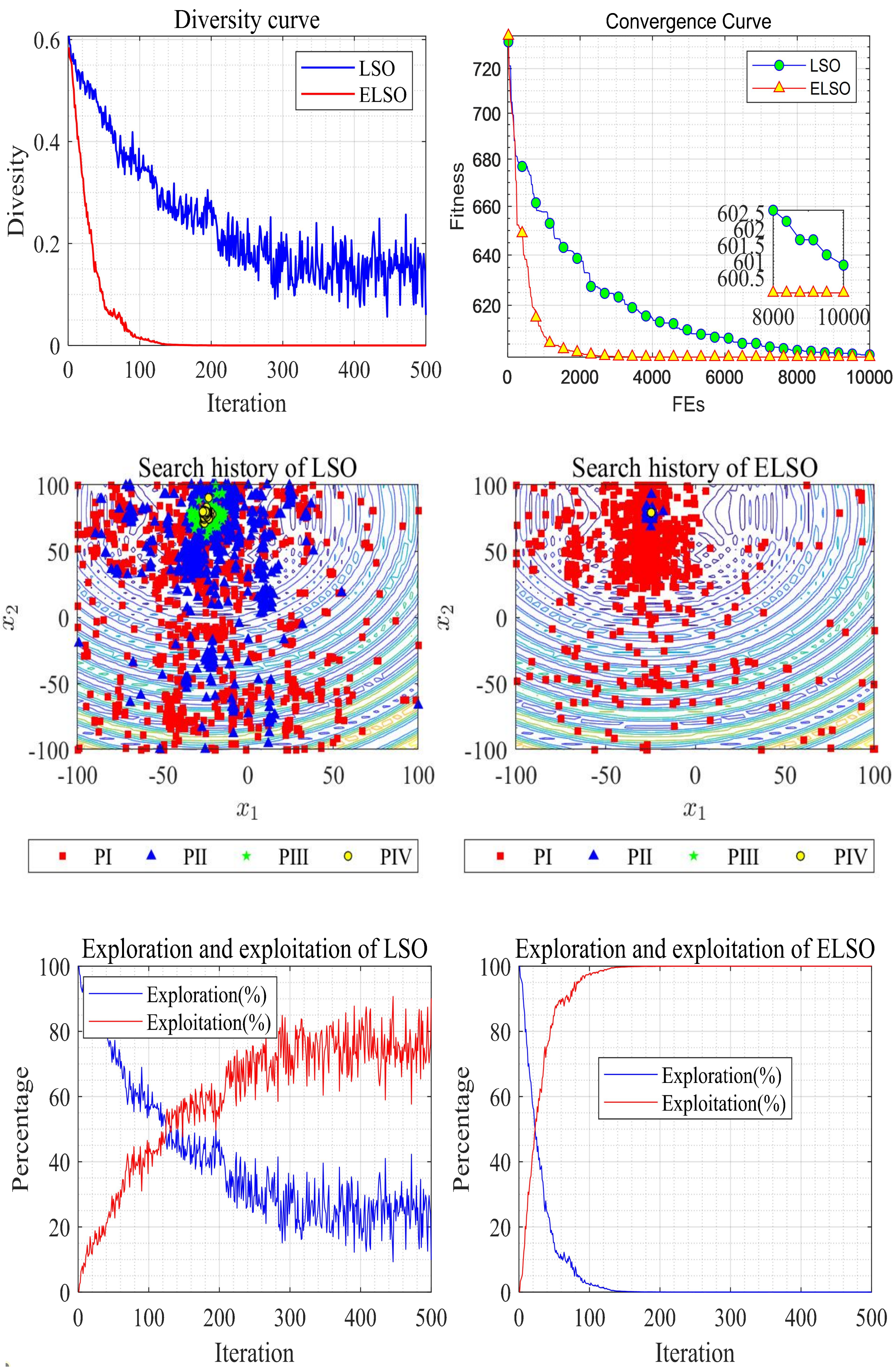

Fig. 6 Qualitative comparison results of f_6

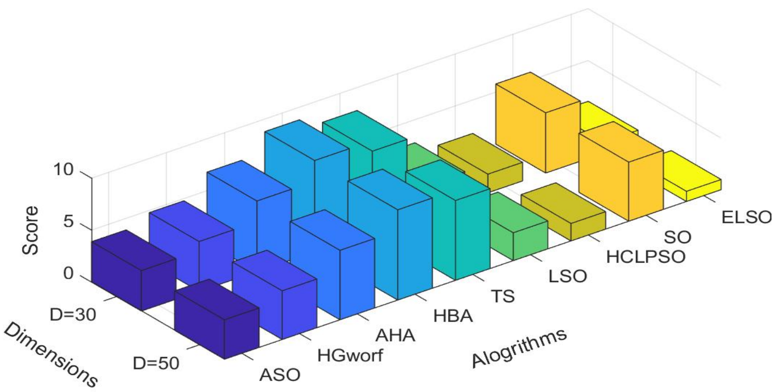

(a) “Mean” indicator

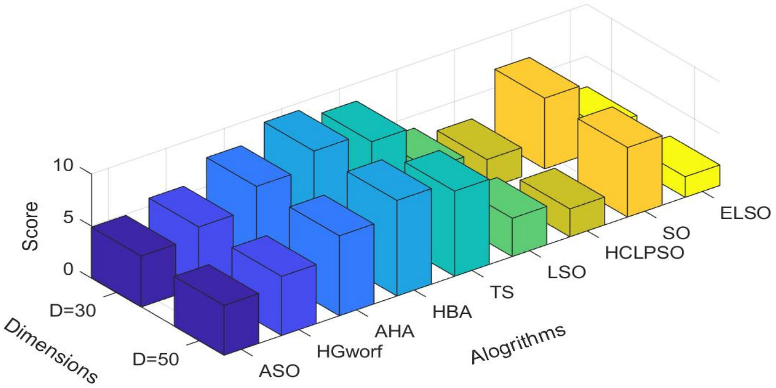

(b) “Std” indicator

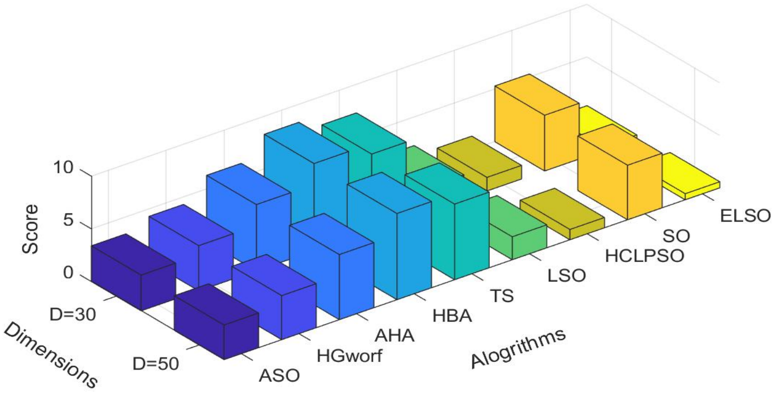

(c) “Best” indicator

Fig. 7 Graphical results of Friedman's test

Among various approaches, the penalty method [24] is one of the most widely used techniques for handling constrained optimization problems. The objective function with the penalty method typically takes the form of the following equation:

$$\min F\left(X,\alpha,\beta\right)=f\left(X\right)+\alpha\sum_{j=1}^{p}\max\{g_j\left(X\right),0\}$$
$$+\beta\sum_{k=p+1}^{m}\left|h_k\left(X\right)\right| \tag{26}$$

Where α and β are penalty factors.

When ELSO is applied to constrained optimization problems, relying solely on fitness-dominated individuals for search guidance shows certain limitations. This approach may not adequately ensure that the population satisfies the constraints. Such shortcomings often lead to premature convergence in infeasible regions that contain constraint-violating solutions. The FDC method addresses this issue in two ways. First, it selects high-fitness leaders. Second, it maintains population diversity by using dual-objective selection criteria in both the decision and constraint spaces. To enhance ELSO's local search effectiveness, the FDC mechanism is incorporated as an enhancement module, specifically strengthening its constraint-handling capability within the hybrid optimization framework defined in Equation (27):

$$X_{i+1}(t)=X_i(t)+\varepsilon RV_1^n GI\left(X_{L1}(t)-X_{L3}(t)\right)$$
$$\times\left(X_{r1}(t)-X_{r2}(t)\right) \tag{27}$$

is changed to:

$$X_{i+1}(t) = X_i(t) + \varepsilon RV_1^n GI\left(X_{L1}(t) - X_{L3}(t)\right) \times\left(X_{r\_FDC}(t) - X_{r2}(t)\right) \tag{28}$$

And

$$X_{i+1}(t) = X_i(t) + \varepsilon RV_1^n GI\left(X_{L2}(t) - X_{L3}(t)\right) \times\left(X_{r3}(t) - X_{r4}(t)\right) \tag{29}$$

is changed to

$$X_{i+1}(t) = X_i(t) + \varepsilon RV_1^n GI\left(X_{L2}(t) - X_{L3}(t)\right) \times\left(X_{r3\_FDC}(t) - X_{r4}(t)\right) \tag{30}$$

The FDC method is integrated into ELSO, forming the enhanced FDC-ELSO variant.

The detailed descriptions of the four optimization problems we selected are as follows：

A. Spring problem

Springs are essential components in mechanical systems and are widely used in automotive, aerospace, and biomedical engineering. The optimization of spring design aims to enhance performance by balancing multiple objectives, including material selection, geometric parameters, and manufacturing processes. The design process must also satisfy several operational constraints, such as stress limits, stiffness requirements, and fatigue resistance. A rigorous mathematical model is detailed in reference [25].

As shown in Table VII, among all algorithms that incorporate the FDC method, the FDC-ELSO algorithm achieves the best performance on the spring design problem. This result indicates that FDC-ELSO is highly competitive in solving constrained optimization problems.

B. Reducer design problem

The gear reducer is a crucial transmission component, widely used across various applications. In this optimization problem, seven design variables are used. The objective is to minimize the reducer's mass while meeting eleven constraints.

The optimized design not only reduces mass but also enhances load-bearing capacity and extends service life. Detailed mathematical modeling can be found in reference [26].

As shown in Table VIII, FDC-ELSO achieves the highest mean value for the reducer design problem and significantly outperforms the other algorithms. This result demonstrates that FDC-ELSO possesses strong optimization capability for this problem and can effectively solve constrained optimization problems.

C. WSN coverage optimization problem

Wireless Sensor Networks (WSNs) consist of distributed sensor nodes. Optimal node deployment is essential for maximizing network coverage [29]. Coverage is defined as the ratio of the monitored area to the total area, the mathematical model for WSN coverage optimization, along with its technical specifications, is detailed in [30].

As shown in Table IX, the ELSO algorithm achieves both the highest mean value and the lowest ranking score, demonstrating its superiority in coverage optimization. ELSO effectively achieves optimal coverage, confirming its outstanding capability in solving unconstrained optimization problems compared to other algorithms.

D. Bridge Arch Design Optimization Problem

In bridge design, optimizing arch structures through topology optimization can enhance efficiency and reduce material usage. This process emphasizes material minimization and geometric refinement to achieve optimal structural performance. The mathematical framework is provided in reference [31].

As shown in Table X, the ELSO algorithm ranks first and exhibits a notably small standard deviation, indicating the excellent stability of its results. This performance not only significantly surpasses that of other algorithms but also demonstrates ELSO's outstanding effectiveness in solving unconstrained optimization problems.

VII. Summary and Outlook

In this study, we propose an Enhanced Light Spectral Optimization Algorithm (ELSO) to address the limitations of the conventional Light Spectral Optimization Algorithm (LSO) and to provide innovative solutions for both unconstrained and constrained optimization problems. ELSO integrates three strategic enhancements: Logistic chaotic mapping, Cauchy mutation, and Lévy flights. These mechanisms work synergistically to balance exploration and exploitation, enhance global search ability to avoid local optima, and reduce premature convergence, thereby improving both optimization accuracy and computational efficiency. We first incorporate the FDC method into ELSO's constraint-handling framework, greatly improving feasibility in constrained optimization. Effectiveness and sensitivity analyses validate component benefits and identify optimal parameters [32]. Comparative results show ELSO surpasses LSO and eight metaheuristics in solution quality and convergence reliability, as supported by the Friedman and Wilcoxon tests. In addition, we rigorously evaluated the optimization capabilities of ELSO and FDC-ELSO through four classical engineering problems, confirming their competitiveness and superior performance in both unconstrained and constrained scenarios.

Although ELSO and FDC-ELSO have demonstrated remarkable results in continuous single-objective optimization problems, their advantages in discrete and multi-objective optimization problems require further validation [33]. In future work, we will systematically introduce advanced enhancement strategies and thoroughly investigate the application of ELSO and FDC-ELSO in discrete and multi-objective optimization. The focus will be on fully unlocking their potential and expanding the applicability of these algorithms to emerging, complex optimization domains [34].

In summary, our primary objective is to meet the diverse and evolving demands of real-world applications by continuously identifying and effectively addressing the current limitations of ELSO, strengthening its theoretical foundation and practical value, and developing multiple optimized versions.

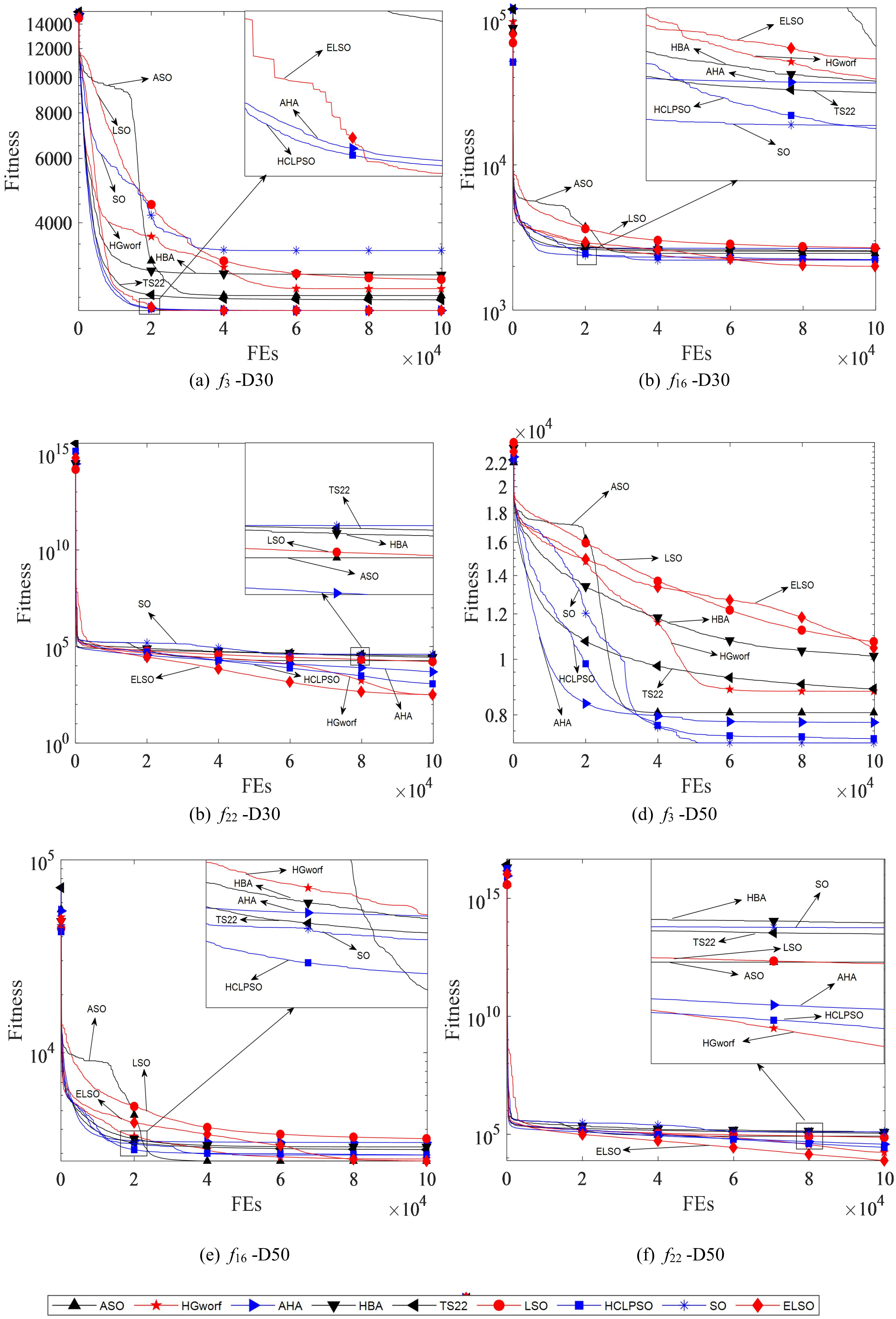

Fig. 8 Convergence curve comparison diagram

TABLE VI. ENGINEERING PROBLEM

No. Problem	Name	Dimension	Reference
P1	Spring problem	3	[25]
P2	Reducer design	7	[26]
P3	WSN coverage optimization	4	[27]
P4	Bridge Arch Design	6	[28]

TABLE VII. SPRING PROBLEM RESULT

Algorithm	Mean	Std	Best	Rank
FDC-ASO	1.2665E-02	6.8050E-13	1.2665E-02	3
FDC-HGworf	1.2674E-02	3.7206E-06	1.2667E-02	6
FDC-AHA	1.2693E-02	2.3069E-13	1.2665E-02	7
FDC-HBA	2.2410E-01	2.7624E-01	1.6890E-02	9
FDC-TS	1.2744E-02	1.2499E-04	1.2700E-02	8
FDC-LSO	1.2665E-02	1.1690E-08	1.2665E-02	5
FDC-HCLPSO	1.2665E-02	7.7780E-18	1.2665E-02	2
FDC-SO	1.2665E-02	1.2586E-08	1.2665E-02	4
FDC-ELSO	1.2660E-02	3.5000E-18	1.2660E-02	1

TABLE VIII. REDUCER DESIGN PROBLEM RESULTS

Algorithm	Mean	Std	Best	Rank
FDC-ASO	1.7249E+00	5.4777E-11	1.7249E+00	4
FDC-HGworf	1.7251E+00	1.2390E-04	1.7249E+00	6
FDC-AHA	1.7249E+00	4.9794E-12	1.7249E+00	3
FDC-HBA	4.0000E+19	4.9827E+19	3.4441E+00	9
FDC-TS	1.8784E+00	1.5651E-01	1.7306E+00	8
FDC-LSO	1.2665E-02	1.1690E-08	1.2665E-02	5
FDC-HCLPSO	1.7249E+00	1.1292E-15	1.7249E+00	2
FDC-SO	1.8700E+00	2.0903E-01	1.7285E+00	7
FDC-ELSO	1.1499E+00	3.5000E-11	1.1499E+00	1

TABLE. IX REDUCER DESIGN PROBLEM RESULTS

Algorithm	Mean	Std	Best	Rank
ASO	1.3025E-02	4.7501E-11	1.2999E-02	3
HGworf	1.2750E-02	9.1200E-05	1.2705E-02	6
AHA	1.2901E-02	3.5503E-12	1.2800E-02	7
HBA	2.4100E-01	3.1500E-01	1.8000E-02	9
TS	1.2840E-02	1.5000E-03	1.2790E-02	8
LSO	1.2950E-02	8.5000E-09	1.2902E-02	5
HCLPSO	1.2667E-02	6.5200E-17	1.2660E-02	2
SO	1.2738E-02	1.1000E-07	1.2655E-02	4
ELSO	1.2620E-02	3.2500E-16	1.2600E-02	1

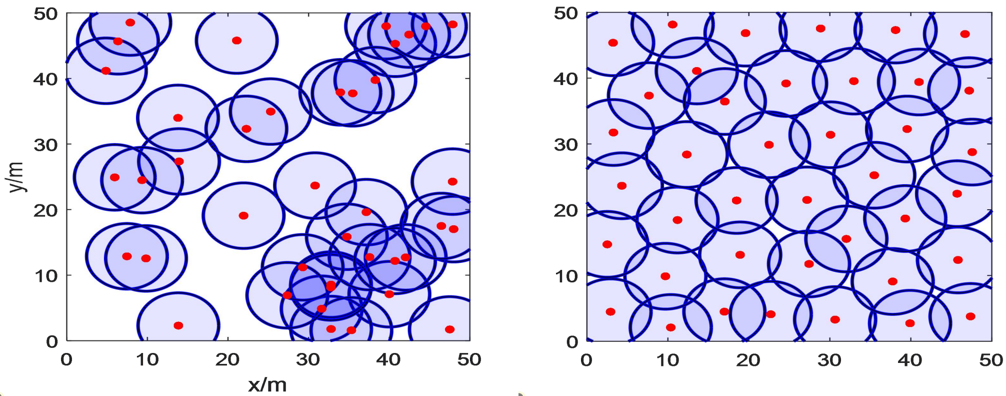

Fig. 9 Initial node deployment and optimization results for the WSN problem

References

[1] Y. Wu. “A survey on population-based metaheuristic algorithms for motion planning of aircraft”. Swarm and Evolutionary Computation, vol. 62, pp. 100844, 2022.

[2] H. Zhang, J. Thompson, M. Gu, et al. “Efficient on-chip training of optical neural networks using genetic algorithm”. ACS Photonics, vol. 8.6, pp. 1662–1672, 2021.

[3] X. Xia, L. Gui, Y. Zhang. “A fitness-based adaptive differential evolution algorithm”. Information Sciences, vol. 549, pp. 116–141, 2021.

[4] Z. Beheshti, U. Transfer. “Function for binary meta-heuristic algorithms”. Applied Soft Computing, vol. 106, pp. 107346, 2021.

[5] A. Basset, Mohamed, et al. "Binary Light Spectrum Optimizer for Knapsack Problems: an improved model". Alexandria Engineering Journal, vol. 67, pp. 609-632,2023.

[6] T. Thulasi, K. Sivamohan. “LSOCSL: light spectrum optimizer-based convolutional stacked long short term memory for attack detection in IoT-based healthcare applications”. Expert Systems with Applications, vol. 232, pp. 120772, 2023.

[7] S. Saber, S. Salem. “An improved light spectrum optimizer for parameter identification of triple diode PV model”. Sustainable Machine Intelligence Journal, vol. 4, pp. 51–67, 2023.

[8] A. Mohamed, R. Mohamed, et al. “Light Spectrum Optimizer: a novel physics-inspired metaheuristic optimization algorithm”. Mathematics, vol. 10, pp. 3466, 2022.

[9] K. Le, D. Le, H. Nguyen, D. Do, N. Ho. “Entropic-gromov wasserstein between gaussian distributions”. International Conference on Machine Learning, vol. 43, pp. 303–315, 2022.

[10] S. Qiu, D. Wang, G. Xu. “Practical and provably secure three factor authentication protocol based on extended chaotic-maps for mobile lightweight devices”. In IEEE Transactions on Dependable and Secure Computing, vol. 42, no. 19, pp. 1338–1351, 2022.

[11] Y. Mao, M. Wang. “High-efficiency rate control for versatile video coding based on composite cauchy distribution”. Computing Research Repository, vol. 32, pp. 2371–2384, 2022.

[12] K. He, Y. Zhang. “EABOA: Enhanced adaptive butterfly optimization algorithm for numerical optimization and engineering design problems”. Alexandria Engineering Journal /Alexandria Engineering Journal, vol. 87, pp. 543–573, 2024.

[13] W. Zhao, L. Wang, Z. Zhang. “Atom search optimization and its application to solve a hydrogeologic parameter estimation problem”. Knowledge-Based Systems, vol. 163, pp. 283-304, 2019.

[14] T. Tzu-Ching, L. Chen, C. Kuo. “A hybrid grey wolf optimization algorithm using robust learning mechanism for large scale economic load dispatch with vale-point effect”. Applied Sciences-Basel, vol. 13, pp. 267–289, 2023.

[15] W. Zhao, L. Wang, S. Mao. “Artificial Hummingbird Algorithm: a new bioinspired optimizer with its engineering applications”. Computer Methods in Applied Mechanics and Engineering, vol. 388, pp. 425–491, 2022.

[16] F. A. Hashim, E. Houssein, K. Houssein, M. Sharma. “Honey Badger Algorithm: new metaheuristic algorithm for solving optimization problems”. Mathematics and Computers in Simulation, vol. 192, pp. 84-110, 2022.

[17] N. subash, M. Ramachandran, S. Vimala, P. Vidhya. “An investigation on tabu search algorithms optimization”. Sri Indu College of Engineering and Technology, vol. 1, pp. 13–20, 2022.

[18] H. Karami, M. Valikhan, S. Farzin. “Flow Direction Algorithm (FDA): a novel optimization approach for solving optimization problems”. Computers Industrial Engineering, vol. 156, pp. 107224, 2021.

[19] S. Molaei, H. Moazen, S. Najjar. “Particle swarm optimization with an enhanced learning strategy and crossover operator”. Knowledge-Based Systems, vol. 215, pp. 106768, 2021.

[20] F. Hashim, A. G. Hussein. “Snake Optimizer: a novel meta-heuristic optimization algorithm”. Knowledge-Based Systems, vol. 242, pp. 108320, 2022.

[21] N. Zeng. “A dynamic neighborhood-based switching particle swarm optimization algorithm”. IEEE Transactions on Cybernetics, vol. 52, pp. 9290-9301, 2022.

[22] J. Wang, Y. K. Wang. “Multi-strategy enhanced snake optimizer for quantitative structure-activity relationship modeling”. Applied mathematical modeling, vol. 132, pp. 531–560, 2024.

[23] A. Deng, S. Kong, C. Liu. “Deep Attentive Belief Propagation: integrating reasoning and learning for solving constraint optimization problems”. NeurIPS, vol. 138, pp.138: 13–29, 2022.

[24] Y. Mao, M. Wu, S. Wang, et al. “The dynamic penalty function method is used to solve constrained optimization problems”. Computer Engineering and Applications, vol. 58, pp. 83-90, 2022.

[25] J. L. J. Pereira, M. Brendon. “A Powerful Lichtenberg Optimization Algorithm: a damage identification case study”. Engineering Applications of Artificial Intelligence, vol. 68, pp. 11075, 2021.

[26] Z. Jiang, L. Liu, Y. Ding. “Knowledge reuse system for reducer design based on UG/KF technology”. Machinery, vol. 46, pp. 19-22, 2008.

[27] C. Guo, Y. Yang, et al. “WSN coverage optimization based on particle swarm optimization”. A New Kind of Science, volume 5, vol. 24, pp. 11086, 2020.

[28] K. Kamil, M. Salamak “Optimization of geometric parameters of arch bridges using visual programming FEM components and genetic algorithm”. Engineering Structures, vol. 241, pp. 112465-112465, 2021.

[29] Z. Fei, B. Li, S. Yang, et al. “A Survey of Multi-Objective Optimization in Wireless Sensor Networks: metrics algorithms and open problems”. SENSORS, vol. 25, pp. 1-18, 2017.

[30] G. Wang, X. Li. “Wireless sensor network coverage optimization using a modified marine predator algorithm”. SENSORS, vol. 25, pp. 1-18, 2025.

[31] H. Cao, Y. Chen, L. Yang. “Hanger pre-tensioning force optimization of steel tied-arch bridges considering operational loads”. Structural and Multidisciplinary Optimization, vol. 63, pp. 867-880, 2020.

[32] G. Dhiman. “SSC: a hybrid nature-inspired meta-heuristic optimization algorithm for engineering applications”. Knowledge-Based Systems, vol. 222, pp. 106926, 2021.

[33] X. Wang, X. Mao, H. Khodaei. “A multi-objective home energy management system based on the internet of things and optimization algorithms”. In Journal of Building Engineering, vol. 33, pp. 101603, 2021.

[34] W. Long, T. Wu, et al. “Parameters identification of photovoltaic models By using an enhanced adaptive butterfly optimization algorithm”. Energy, vol. 229, pp. 120–133, 2021.

[35] X. Zhang, T, Yang. “Improved particle swarm algorithm for logistics distribution path optimization”. Atlantis Highlights in Engineering Proceedings of the 2023 8th International Conference on Engineering Management (ICEM 2023), vol. 69, pp. 353-363, 2023.

[36] W. Shan, X. He, H. Liu. “Cauchy Mutation Boosted Harris Hawk Algorithm: optimal performance design and engineering applications”. Journal of Computational Design and Engineering, vol. 10, pp. 503-526, 2023.

[37] J. Yan, G. Hu, B. Shu. “MGCHMO: a dynamic differential human memory optimization with cauchy and gauss mutation for solving engineering problems”. Advances in Engineering Software, vol. 198, pp. 20-24,2024.

[38] P. Cao, Q. Huang. “Hybrid multi-strategy improved butterfly optimization algorithm”. Applied Sciences, vol. 107, pp. 14-24, 2024.

[39] S. K. Joshi. “Lévy flight incorporated hybrid learning model for gravitational search algorithm”. Knowledge-Based Systems, vol. 265, pp. 12860, 2023.